Electronic Supplementary Material (ESI) for Journal of Materials Chemistry C.

Electronic Supplementary Information

Trap-Dominated Nitrogen Dioxide and Ammonia Responses of Air-Stable *p*-channel Conjugated Polymers from Detailed Bias Stress Analysis

Tushita Mukhopadhyaya and Howard E. Katz*

Department of Materials Science and Engineering and Department of Chemistry, Johns Hopkins University, 206 Maryland Hall, 3400 North Charles Street,

Baltimore, Maryland 21218, United States

*corresponding author: email hekatz@jhu.edu

		hours) and t=5 mins represents the transfer curve post exposure to 10 ppm of NO_2 for 5 minutes. (h) **PF4** (control, no bias stress, direct exposure, where t=0 mins represents transfer curve without the application of any gate bias, t=5 mins represents transfer curves after exposure to 10 ppm of NO_2 for 5 mins) (i) **P6** (t=0 mins represents the transfer curve after completion of recover in air ~12 hours) and t=5 mins represents the transfer curve post exposure to 10 ppm of NO_2 for 5 minutes. (j) **P6** (control, no bias stress, direct exposure, where t=0 mins represents transfer curve without the application of any gate bias, t=5 mins represents transfer curves after exposure to 10 ppm of NO_2 for 5 mins. Condition: V_G=V_D=-80 V. *The responses have been monitored at V_G=-80 V (from transfer curves). Please note that we have provided the transfer curves for only the best device. The response data are an average from 10 devices, each from a different film*	
34	**Figure S26**	Responses to NO_2 (10 ppm). For every polymer, the first set represents responses after completion of the air aided recovery after gate bias application (V_G=V_D=-80 V) while the second set represents responses of independent devices not subjected to gate bias and direct exposure to NO_2. For both the cases in case of each polymer, the exposure time was 5 minutes. *Responses are monitored at V_G=-80 V.*	30
35	**Table S8**	Statistical calculation of t and p-values for the case in **Figure S26**.	30
36	**Figure S27**	Changes in V_{th} and μ at t=0 mins (initial transfer characteristic), at t=300 mins (immediately after bias stress) and after continuous exposure to NO_2 to aid the recovery process. The recovery times are mentioned in the text.	30
37	**Figure S28**	Transfer curves showing air aided recovery from gate bias (V_G=V_D=-80 V) for (a) **PF1** (b) **PF2** (c) **PF3** (d) **PF4** and (e) **P6** respectively. 16 mins, 25 mins, 18 mins, 15 mins, 10 mins for **PF1-P6** were the exposure times in air, respectively. The recovery can be explained	31,32

		as follows. Since organic semiconductors are permeable to water, water molecules can also reach the SiO_2 surface in the presence of an organic semiconductor. In this reaction, holes in the semiconductor are converted into proton which can be converted back into holes along with production of H_2. The reversible motion of protons in SiO_2 has been demonstrated by memory effects occurring in $Si/SiO_2/Si$ devices, where protons move through the SiO_2 from one Si layer to the other. In the presence of water, holes in the organic semiconductor, indicated below by OS+, can be converted into protons in the electrolytic reaction $2H_2O + 4OS^+ \rightarrow 4H^+ + O_2(g) + 4OS$, where OS refers to electrically neutral sites in the organic semiconductor. Next, protons can be converted back into holes in the reaction $2H^+ + 2OS \rightarrow 2OS^+ + H_2$ (g). There will be an equilibrium between the surface density $[OS^+]$ of holes in the semiconductor and the volume density $[H^+]$ of protons in the oxide at the interface with the semiconductor, leading to the linear relation $[H^+] = \alpha[OS^+]$, where the parameter α is a proportionality constant, which is determined by the reaction constants. Systematic tailoring of molecular and microstructural features determines the degree of shift in V_{th} as well as recovery. Further at such high voltages; less mobile states are accessible due to increase in microstructural disorder (created along with inherent traps) causing more shallow traps. During recovery, under application of a zero gate bias the transfer curve of a transistor that has suffered from bias stress shifts back to the transfer curve before the bias stress.	
38	**Figure S29**	Changes in V_{th} and μ at t=0 mins (initial transfer characteristic), at the '**trap create**' time t=300 mins (immediately after bias stress) and after continuous **exposure to air** to aid the recovery process. The times for which the stressed devices were exposed to air (already mentioned in the main text) are 16, 25, 18, 15, 10 minutes.	32
39	**Figure S30**	Transfer curves showing the effect of NH_3 gas (10 ppm) immediately after applying gate bias (V_G=V_D=-80 V) for (a) **PF1** (b) **PF2** (c)	33

		PF3 (d) **PF4** and (e) **P6** respectively. The percentages are calculated at V_G=-80 V. The exposure times are:16 mins for **PF1**, 25 mins for **PF2**, 18 mins for **PF3**, 15 mins for **PF4** and 10 mins for **P6**.	
40	**Figure S31**	Changes in V_{th} and μ as an effect of NH_3 gas (10 ppm) immediately after applying gate bias (V_G=V_D=-80 V) for (a) **PF1** (b) **PF2** (c) **PF3** (d) **PF4** and (e) **P6** respectively. The percentages are calculated at V_G=-80 V. The exposure times are:16 mins for **PF1**, 25 mins for **PF2**, 18 mins for **PF3**, 15 mins for **PF4** and 10 mins for **P6**.	34
41	**Figure S32**	Transfer curves under ambient air (t=0 mins), post application of trap erase protocol [(i) (V_G=V_D=-80 V) and (ii) V_G = +80 V, V_D =0 V] followed by (a) 10 ppm NO_2 exposure for **PF1** (b) 10 ppm NH_3 exposure for **PF1** (c) ambient air exposure for **PF1** (d) 10 ppm NO_2 exposure for **PF2** (e) 10 ppm NH_3 exposure for **PF2** (f) ambient air exposure for **PF2** (g) 10 ppm NO_2 exposure for **PF3** (h) 10 ppm NH_3 exposure for **PF3** (i) ambient air exposure for **PF3** (j) 10 ppm NO_2 exposure for **PF4** (k) 10 ppm NH_3 exposure for **PF4** (l) ambient air exposure for **PF4** (m) 10 ppm NO_2 exposure for **P6** (n) 10 ppm NH_3 exposure for **P6** (o) ambient air exposure for **P6**. The exposure times are 16 mins for **PF1**, 25 mins for **PF2**, 18 mins for **PF3**, 15 mins for **PF4** and 10 mins for **P6**. Please note that only transfer curves for the best devices are shown; however, quantitative evaluation is done from 10 devices from independent, different films of every material.	35
42	**Table S9**	Trends in ΔV_{th} (V) and percent change of μ ($cm^2V^{-1}s^{-1}$) from reverse bias stress	36
43	**Figure S33**	V_{th} and μ changes under ambient air (t=0 mins), post application of trap erase protocol [(i) (V_G=V_D=-80 V) and (ii) V_G = +80 V, V_D =0 V] followed by 10 ppm NO_2 exposure for (a) **PF1** (b) **PF2** (c) **PF3** (d) **PF4** (e) **P6.** The exposure times are 16 mins for **PF1**, 25 mins for **PF2**, 18 mins for **PF3**, 15 mins for **PF4** and 10 mins for **P6**	37

44	**Figure S34**	Change in I_{DS} (%) monitored at V_G=-80 V after trap erase. **P6** has highest mobility; so at V_G=-80 V, the current is the highest.	37
45	**Figure S35**	V_{th} and μ changes under ambient air (t=0 mins), post application of trap erase protocol [(i) (V_G=V_D=-80 V) and (ii) V_G = +80 V, V_D =0 V] followed by 10 ppm NH_3 exposure for (a) **PF1** (b) **PF2** (c) **PF3** (d) **PF4** (e) **P6.** The exposure times are 16 mins for **PF1**, 25 mins for **PF2**, 18 mins for **PF3**, 15 mins for **PF4** and 10 mins for **P6.**	38
46	**Figure S36**	Transfer curves under ambient air (t=0 mins), and on exposure to 10 ppm of NH_3 (a) **PF1** (b) **PF2** (c) **PF3** (d) **PF4** (e) **P6.** This is a direct exposure of unstressed devices. These are the controls used for the trap erase experiments. The exposure times are 16 mins for **PF1**, 25 mins for **PF2**, 18 mins for **PF3**, 15 mins for **PF4** and 10 mins for **P6**	39
47	**Figure S37**	V_{th} and μ changes under ambient air (t=0 mins), post application of trap erase protocol [(i) (V_G=V_D=-80 V) and (ii) V_G = +80 V, V_D =0 V] followed by air exposure for (a) **PF1** (b) **PF2** (c) **PF3** (d) **PF4** (e) **P6.** The exposure times are 16 mins for **PF1**, 25 mins for **PF2**, 18 mins for **PF3**, 15 mins for **PF4** and 10 mins for **P6**	39

Materials and Methods: Unless otherwise indicated, the starting materials were obtained from Sigma-Aldrich or Alfa Aesar and were used without further purification. **P6** was obtained from Ossila. The GPC and other structural characterization data are provided therein. ^{1}H NMR (300 MHz) spectra were recorded on a Bruker Advance spectrometer using $CDCl_3$ as solvent and tetramethylsilane (TMS) as the internal standard. Molecular weights were determined using gel permeation chromatography on a Waters 1515 Isocratic HPLC with a Waters 2489 Refractive Index (**RI**) and UV/vis detector using polystyrene as standard and THF as eluent. Cyclic voltammetry (CV) was performed in a one-chamber, three-electrode cell in acetonitrile containing 0.1 M *n*-Bu_4NPF_6 as a supporting electrolyte. A glassy carbon disk, a platinum wire and Ag/AgCl electrode, were used as the working electrode, auxiliary electrode and reference electrode, respectively. The supporting electrolyte was stored with molecular sieves to keep it dry. The efficient film area on work electrode is 3.1 mm^2 and the film thickness was 2 ~ 3 μm. Atomic force microscopy images were taken in tapping mode using a Dimensional 3100 AFM (Bruker Nano, Santa Barbara, CA). The images were visualized using the Nanoscope software (Bruker). Gas sensing experiments were conducted using the Environics 4040 Series Gas Dilution System.

Calculation of HOMO Level: Ferrocene/ferrocenium (Fc/Fc^+) was used as the external reference. The redox potential of Fc/Fc^+ was assumed to have an absolute energy level of -4.80 eV to vacuum. The redox potential of Fc/Fc^+ was measured under the same conditions, and was found to be 0.03V vs Ag/AgCl. Energy levels of the highest occupied molecular orbital (HOMO) were calculated according to the equations: HOMO = -e(E_{ox}+ 4.64) (eV), where E_{ox} is the onset oxidation potential vs Ag/AgCl.

OFET *Fabrication and Characterization*: Top contact/bottom gate ***OFET*** devices were fabricated by using *n*-doped silicon wafers with 300 nm silicon dioxide as substrates. The substrates were cleaned and modified with hexamethyldisilazane (HMDS) self-assembled monolayer. The polymers were dissolved in chloroform with at concentration of 10 mg mL^{-1}. The thin films were prepared by spin coating the solution on the substrates. The polymer thin-films were then annealed on a hot plate at 120 °C for 10 min under N_2 atmosphere. Gold contacts of 50 nm were deposited on the thin film as source and drain electrodes with a channel width of 1.1 cm and a channel length of 200 μm. The electrical performance of

transistors before and after exposure to gas was carried out using an Agilent 4155C Semiconductor Parameter analyzer in ambient at a constant swipe rate of 0.5 Vs^{-1}. The mobility was calculated in the saturation regime according to the equation: $I_{DS} = (W/2L)\mu C_i(V_G - V_T)^2$, where I_{DS} is the drain current, μ is the mobility, and V_G and V_T are the gate voltage and threshold voltage, respectively. The bias stress experiments were carried out for a total sampling time of 18,000 seconds at an interval of 3 seconds for each I_{DS} (A) reading. The compliance was set to 10 mA. The gate and drain voltages were held constant at -80 V for this time. The gate bias equation $\Delta V_{th} = (V_{th,0}-V_{G,bias})[1-\exp\{-(t/\tau)^{\beta}\}]$ was rearranged as $\log[\ln(1-\Delta V_{th}/V_0)] = \beta \log t - \beta \log \tau$, where $V_0=(V_{th,0}-V_{G,bias})$. The values of β and τ were obtained from slope and intercept respectively.

Sensing Measurement: A home-made gas flow chamber was used for NO_2 and NH_3 exposure experiments. The chamber was blown by air (humidity of 46%) for 10 min before the devices were placed inside. NO_2 and NH_3 gas and air were introduced through clean tubing and flowed through the Environics 4040 Series Gas Dilution System to obtain desired concentration, directly on the devices at the probe station and sensitivities were thus measured by a continuous flow method. The percentage drifts in air were measured by swiping the gate voltage at a constant rate of 0.5 V/s for a fixed period of time (5 mins).

Synthesis and Characterizations:

PF1 to PF4 were synthesized according to the sequences shown in **Figure S1** using previously reported literature procedures while **P6** was obtained commercially. The detailed synthetic methods and characterization is already shown in our previous work. We show the characterization results (^{1}H NMR, Gel Permeation Chromatography) here again for easy reference. [1,2]

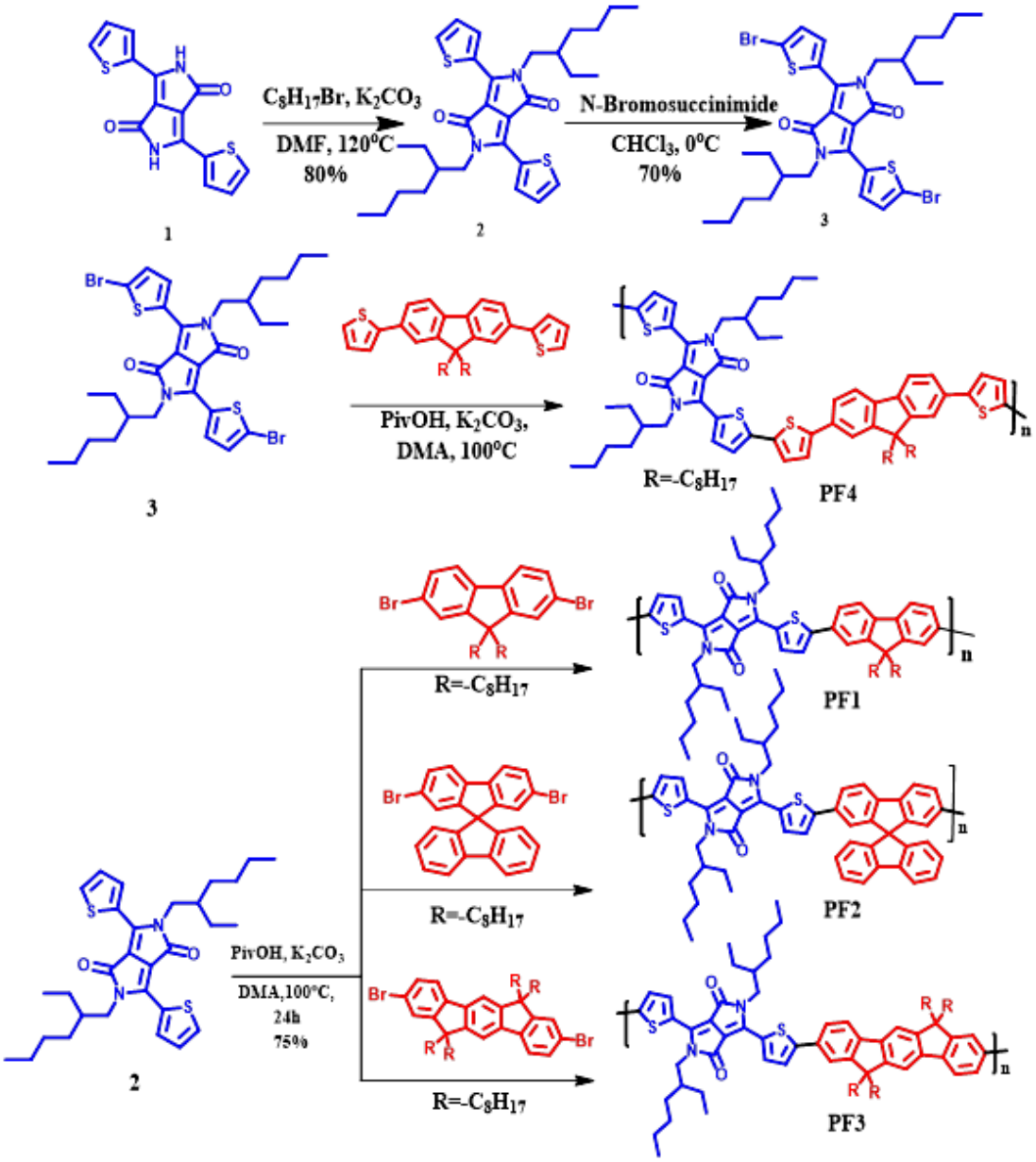

Figure S1. Synthetic scheme for **PF1-PF4**. **P6** is obtained commercially.

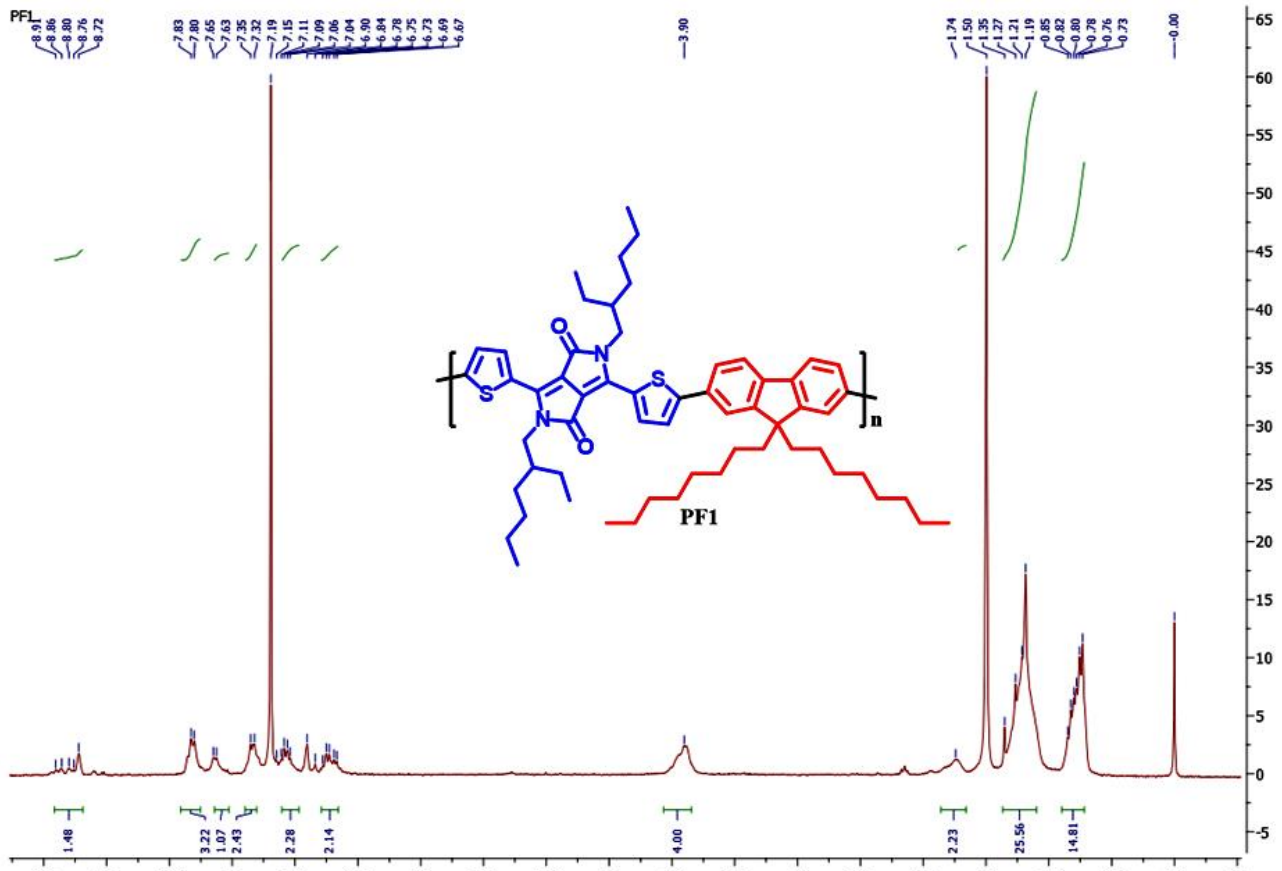

Figure S2. ^{1}H NMR of **PF1**. ^{1}H NMR ($CDCl_3$, 300 MHz) δ8.69 (m, 2H), 8.00-6.75(m, 7H), 4.0 (s, 4H), 1.75 (m, br, 2H), 1.75 (m, 25H), 0.75 (m, 18H)

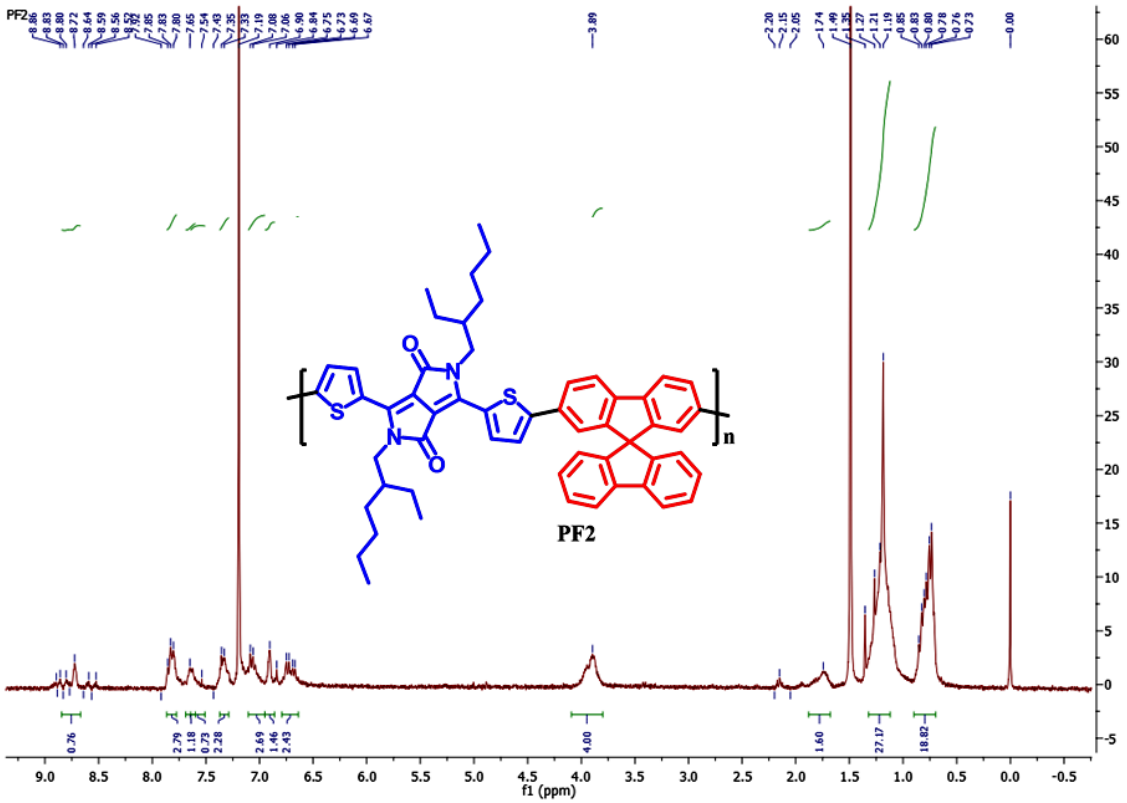

Figure S3. ^{1}H NMR of **PF2.** ^{1}H NMR ($CDCl_3$, 300 MHz) δ 9.0-8.5 (m, 1H), 8.0-6.5 (m, 16H), 4.0 (m, 4H), 1.75 (m, br, 2H), 1.25 (m, 27H), 0.75(m, 18H)

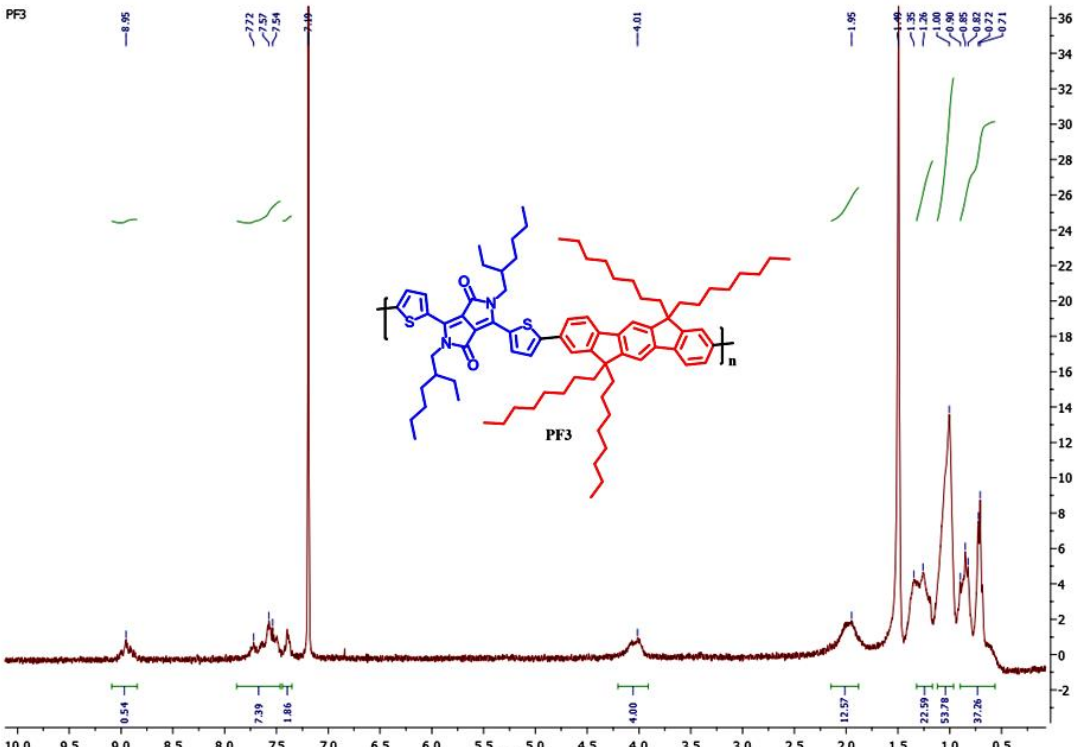

Figure S4. ^{1}H NMR of **PF3**.^{1}H NMR ($CDCl_3$, 300 MHz) δ 9.0 (m, 1H), 8.0-7.0 (m, 10H), 4.0 (m, 4H), 2.0 (m, 2H), 1.25 (m, 28H), 0.75 (m, 18H)

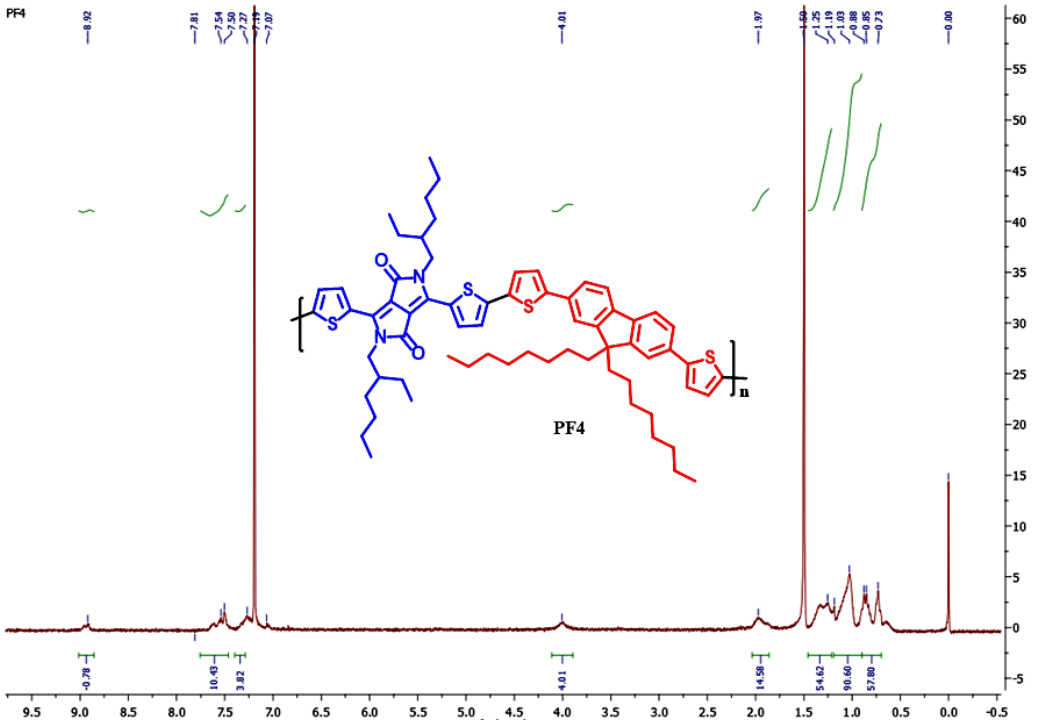

Figure S5.^{1}H NMR of **PF4**.^{1}H NMR ($CDCl_3$, 300 MHz), δ 9.0 (m, 2H), 8.0-7.0 (m, 12H), 4.0 (m, 4H), 2.0 (m, 2H), 1.25 (m, 54H), 0.75 (m, 12H)

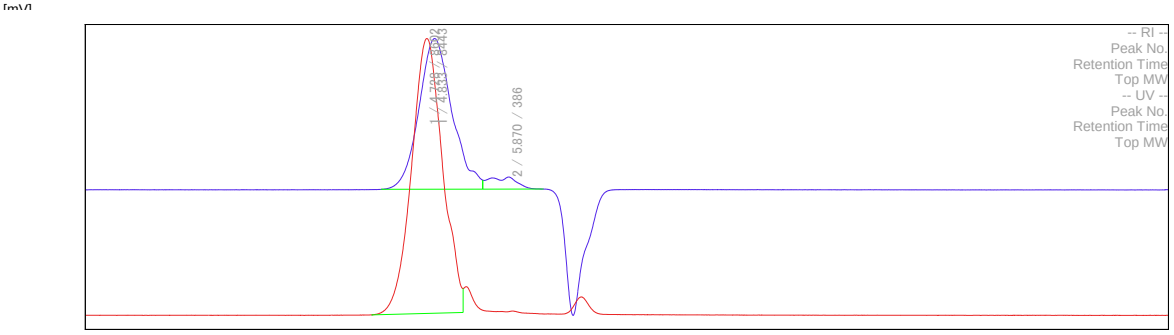

Figure S6. GPC profile of **PF1**

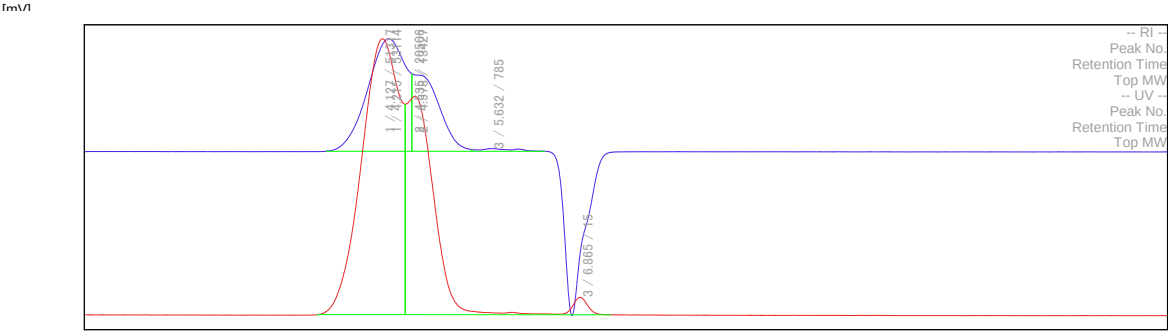

Figure S7. GPC profile of **PF2**.

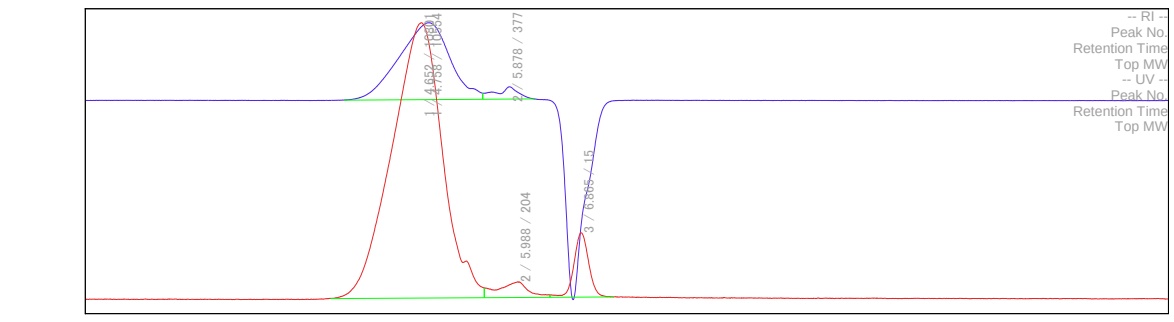

Figure S8. GPC profile of **PF3**.

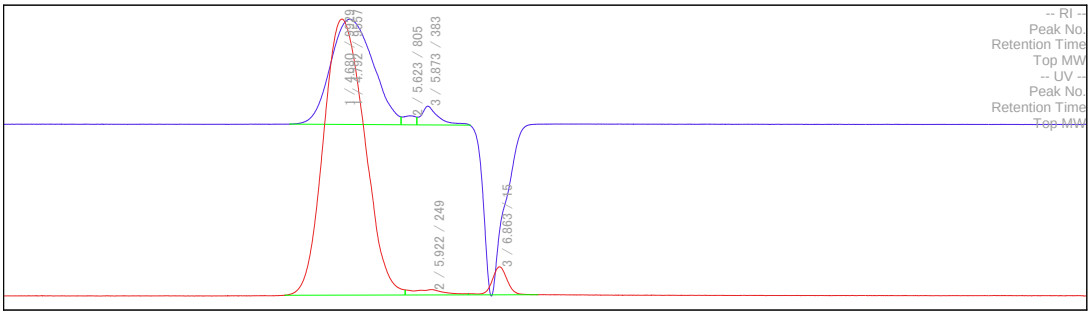

Figure S9. GPC profile of **PF4**.

Table S1. Summary of GPC

Polymer	M_w	M_n	M_w/M_n (PDI)
PF1	10048	7027	1.4
PF2	7351	4407	1.7
PF3	10443	4177	2.5
PF4	2444	2049	1.1

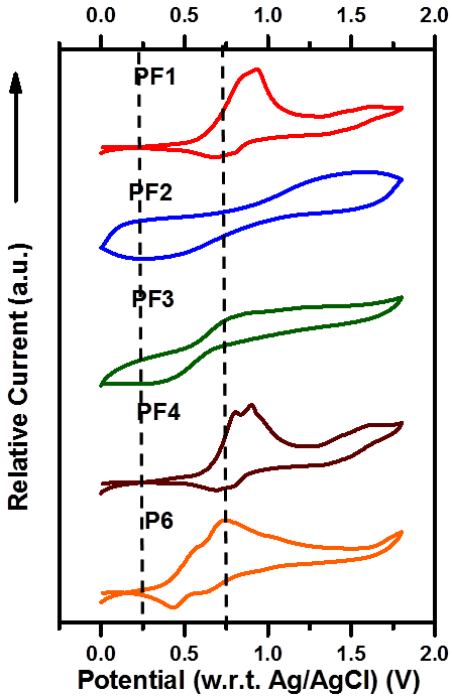

Figure S10. Cyclic voltammograms (oxidation window) of **PF1-PF4** & **P6** adapted from reference 1

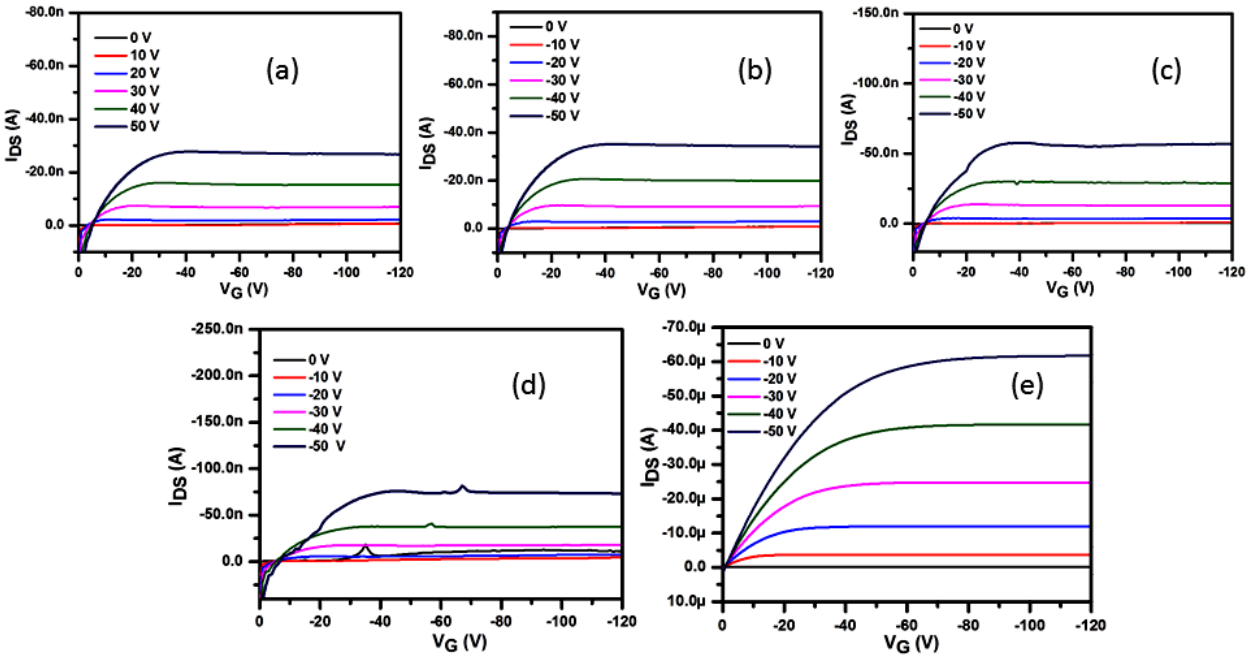

Figure S11. Output curves of (a) **PF1** (b) **PF2** (c) **PF3** (d) **PF4** and (e) **P6**

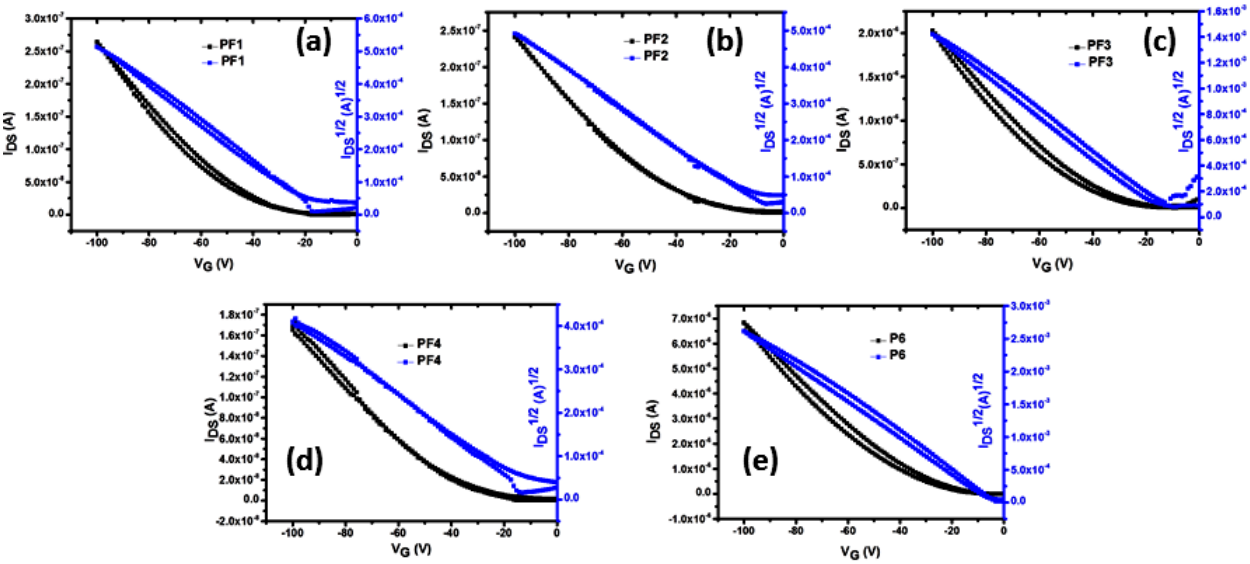

Figure S12. Transfer curves for (a-d) **PF1-PF4** and (e) **P6**

Table S2. Hole mobilities and threshold voltages of polymers

Polymers	μ ($cm^2V^{-1}s^{-1}$)	V_{th} (V)	$V'=V_{th}-40$ (V)
PF1	$(1.26x10^{-4}) \pm (7.20x10^{-6})$	-9.22±3.15	-49
PF2	$(1.00x10^{-4}) \pm (1.02x10^{-5})$	-7.40±1.43	-47
PF3	$(1.20x10^{-3}) \pm (7.32x10^{-4})$	-6.33±1.37	-46
PF4	$(1.98x10^{-4}) \pm (1.40x10^{-5})$	-9.98±0.62	-49
P6	$0.12 \pm (1.97x10^{-2})$	7.38±2.24	-33

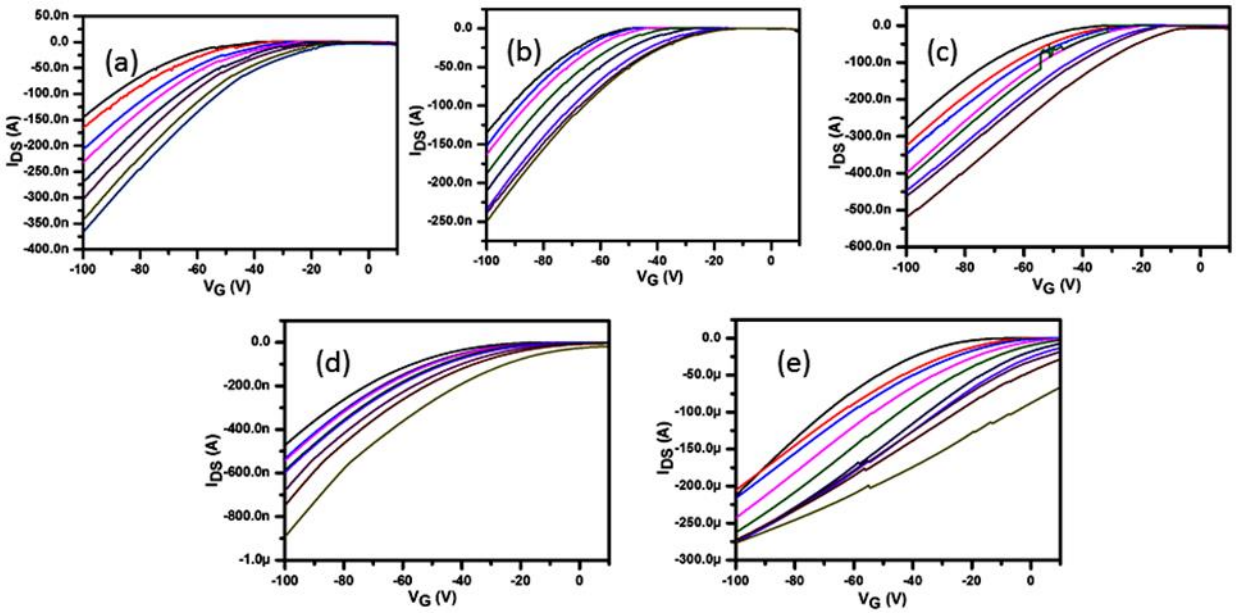

Figure S13. Transfer curves (a) **PF1** (b) **PF2** (c) **PF3** (d) **PF4** (e) **P6** of the best performing device on systematic exposure to 0, 0.5, 1, 2, 3, 5, 7, 10, 15, 20 ppm of NO_2 gas for 5 mins. Note that the values reported are an average from 6 devices with standard errors. Also shown are the series of 25 transfer curves taken before the vapor responses for the same respective polymers. Note that except for **PF2**, the drifts to lower current caused by dynamic bias stress are smaller than the drifts to higher current caused by the response to NO_2.

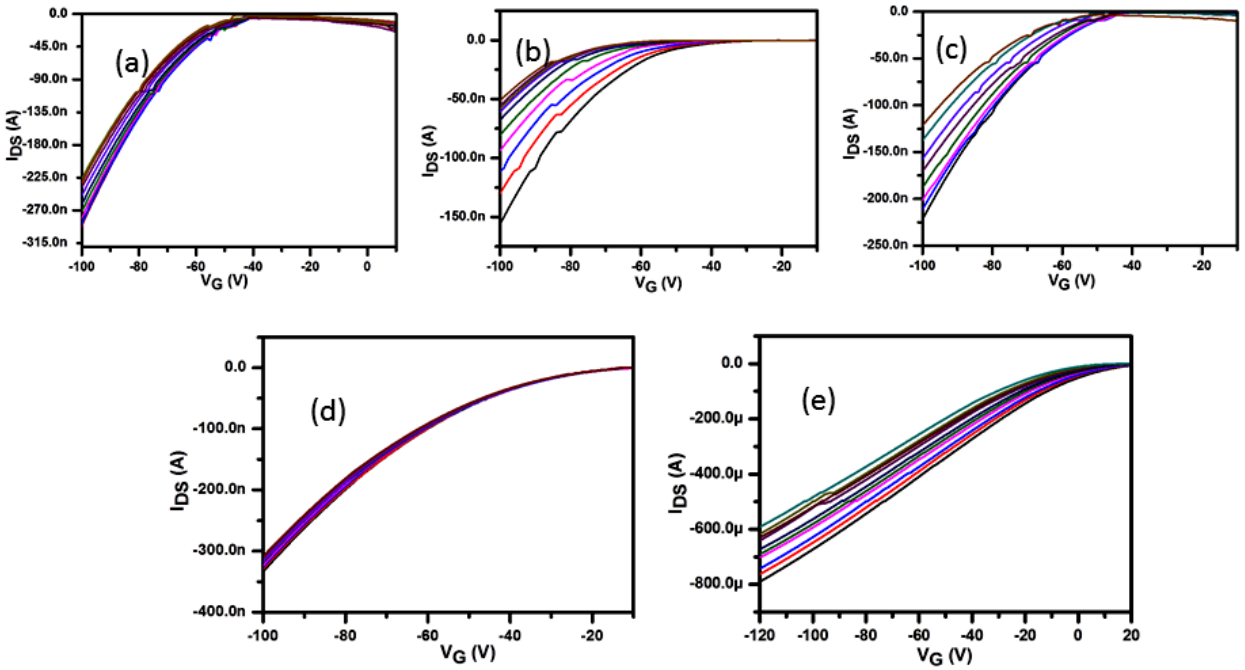

Figure S14. Transfer curves (a) **PF1** (b) **PF2** (c) **PF3** (d) **PF4** (e) **P6** of the best performing device on systematic exposure to 0, 0.5, 1, 2, 3, 5, 7, 10, 15, 20 ppm of NH_3 gas for 5 mins. Note that the values reported are an average from 10 devices with standard errors.

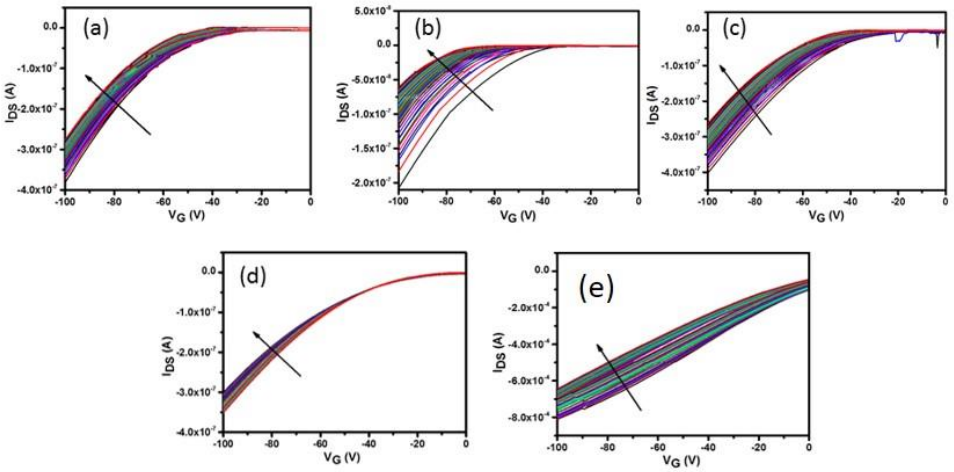

Figure S15. Drifts for 25 mins (cycle test/dynamic bias stress) for (a) **PF1** (b) **PF2** (c) **PF3** (d) **PF4** (e) **P6.** 25 cycles are shown and the last 5 cycles (each cycle taking ~1 minute) are used to calculate the signal-to-noise ratio "D"

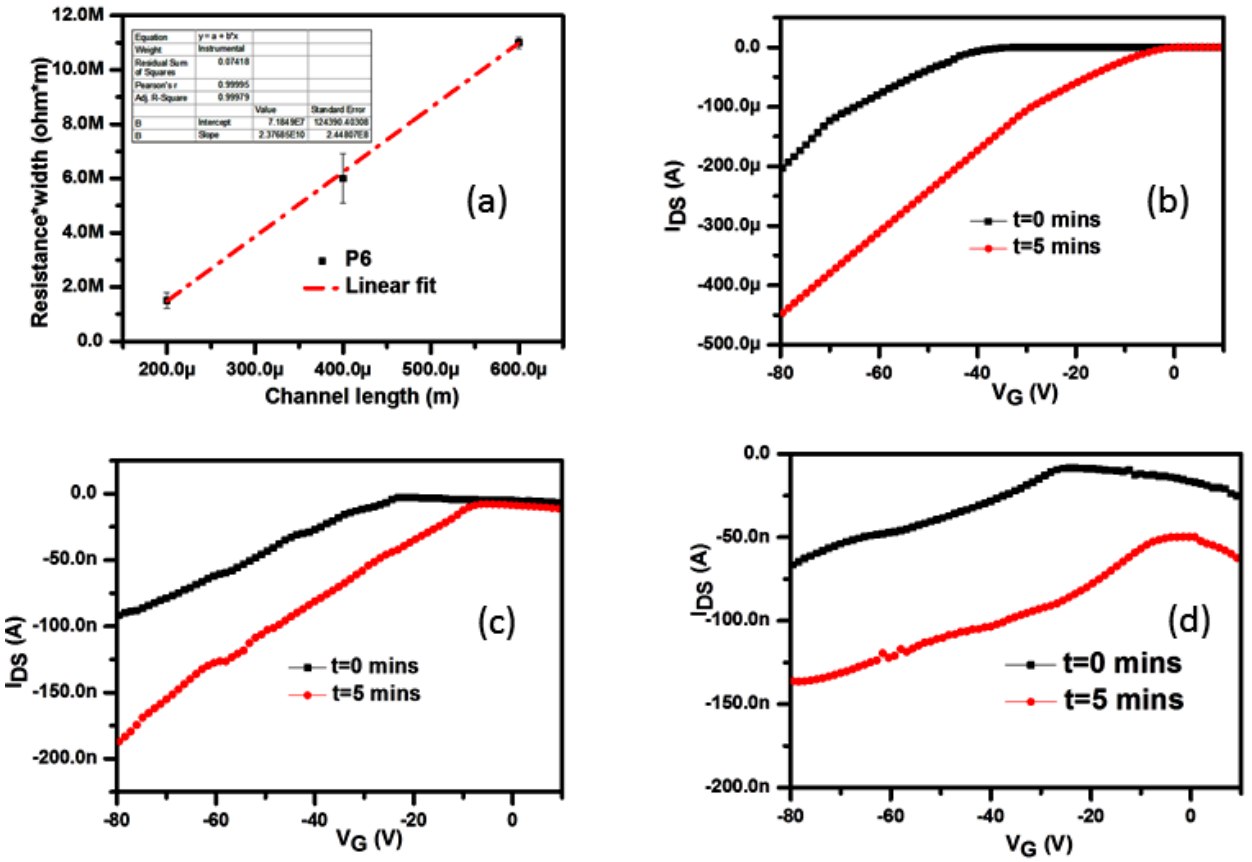

Figure S16. (a) Plot of (total resistance)*(channel width=1.1 cm) versus channel length for **P6**. The error bars are extracted from 3 independent devices. The value of the intercept indicates the contact resistance. (b) t=0 mins represents the initial transfer curve while t=5 mins represents the transfer curve after exposure to 10 ppm of NO_2 gas; for channel length of **200 µm.** (c) t=0 mins represents the initial transfer curve while t=5 mins represents the transfer curve after exposure to 10 ppm of NO_2 gas; for channel length of **400 µm.** (d) t=0 mins represents the initial transfer curve while t=5 mins represents the transfer curve after exposure to 10 ppm of NO_2 gas; for channel length of **600 µm.** The average response is 170±20 %.

It can be seen that the I_{DS} (A) decreases with the increase in length of the channel at a constant width. If monitored at V_G=-80 V; for (a) length=200 µm, I_{DS} = 200 µA (b) length=400 µm, I_{DS} = 99 µA (c) length=600 µm, I_{DS} = 70 µA.

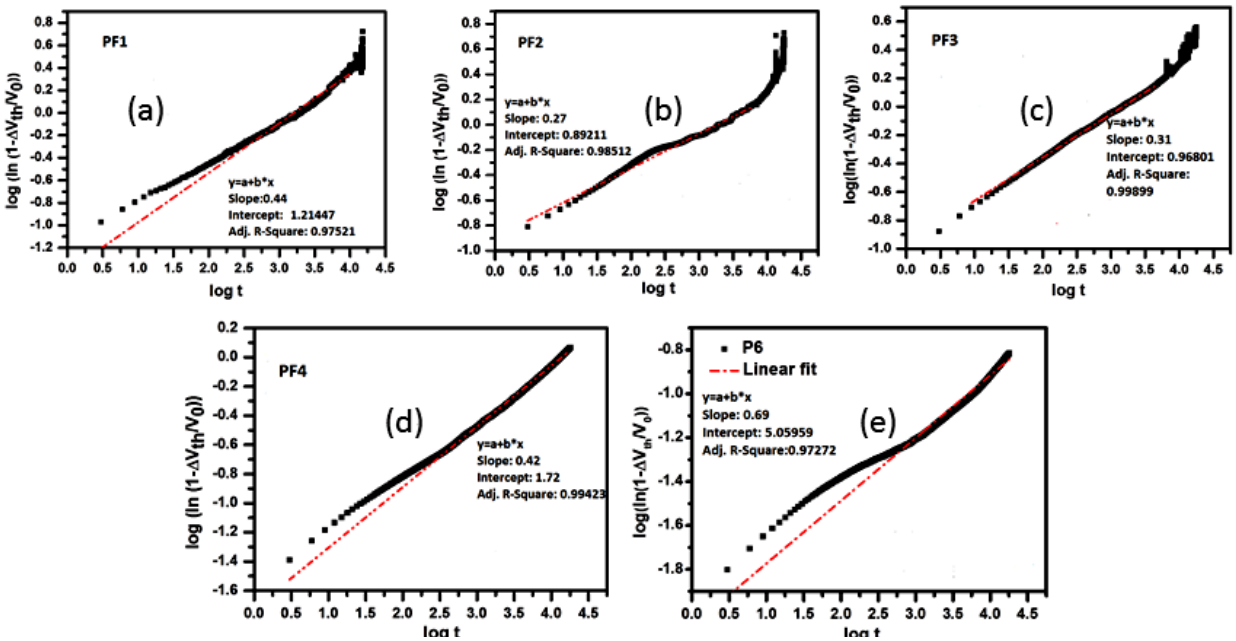

Figure S17. Plots of straight line fits of $\log[\ln(1-\Delta V_{th}/V_0)]$ versus log t for extracting β and τ. Slope indicates β and τ is expressed as $10^{|\text{intercept}|/\text{slope}}$.

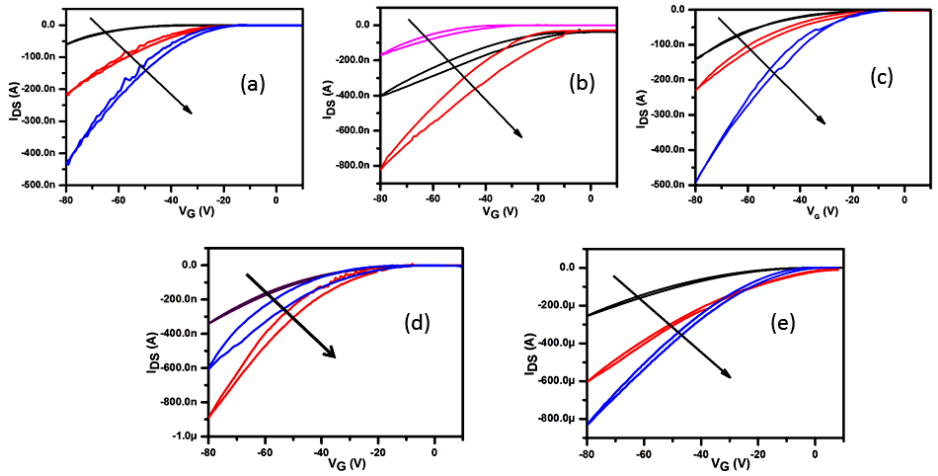

Figure S18. Plots of I_{DS} (A) versus V_G at three temperatures 294, 323 and 373 K for polymers **PF1-PF4 (a-d)** and **P6 (e)**

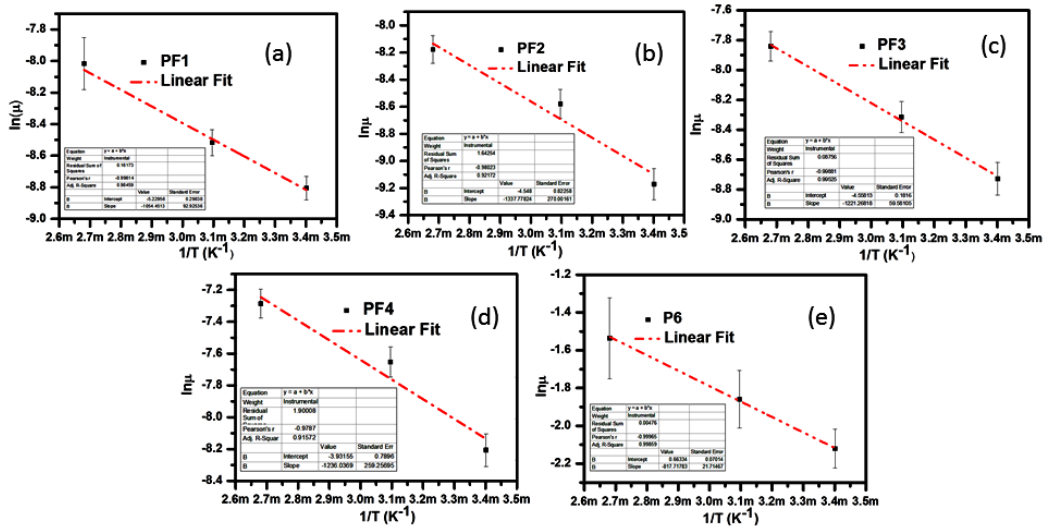

Figure S19. Fits of lnμ versus 1/T (K^{-1}) to elucidate the E_a values

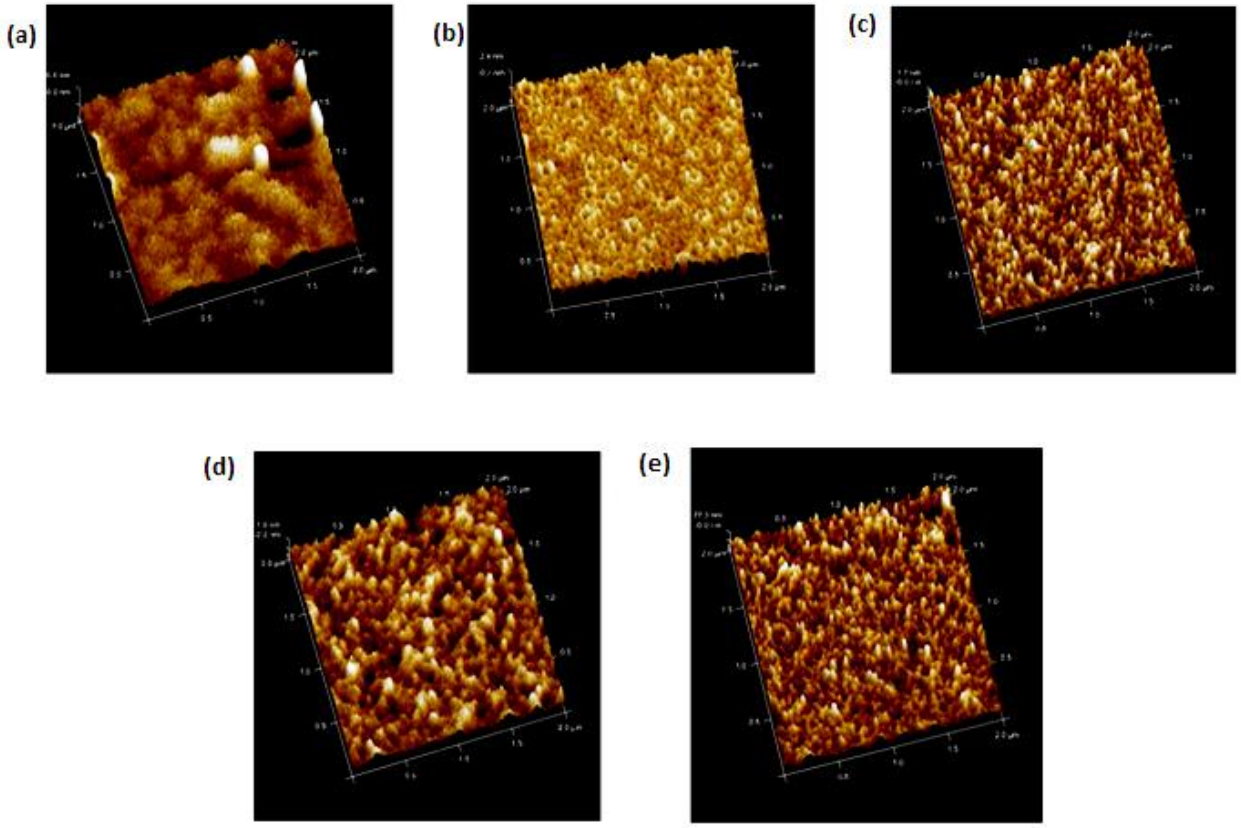

Figure S20. Atomic Force Microscopy (**AFM**) images for (a-d) **PF1-PF4** and (e) **P6.** Scale bar is 2.0 μm.

Table S3. Parameters extracted from temperature-dependent gate bias studies

Polymers	E_a (eV)	lnν	ν (s^{-1})
PF1	0.5	9.36	1.2E4
PF2	0.4	9.8	1.8E4
PF3	0.3	3.7	40
PF4	0.3	5.7	299
P6	0.2	0.1	1.105

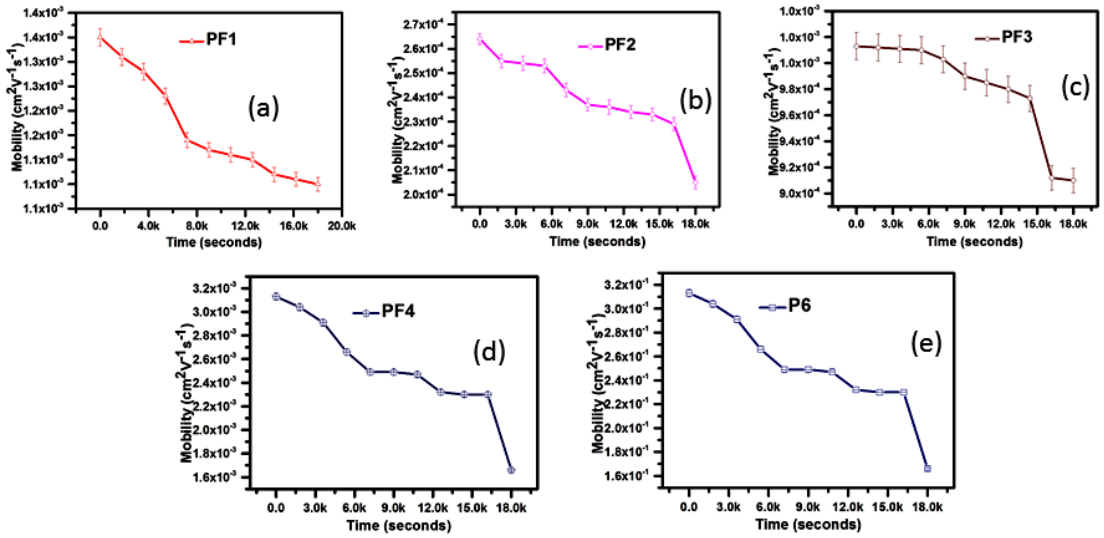

Figure S21. Mobility changes for (a)-(e) (**PF1-P6**) during the bias stress process

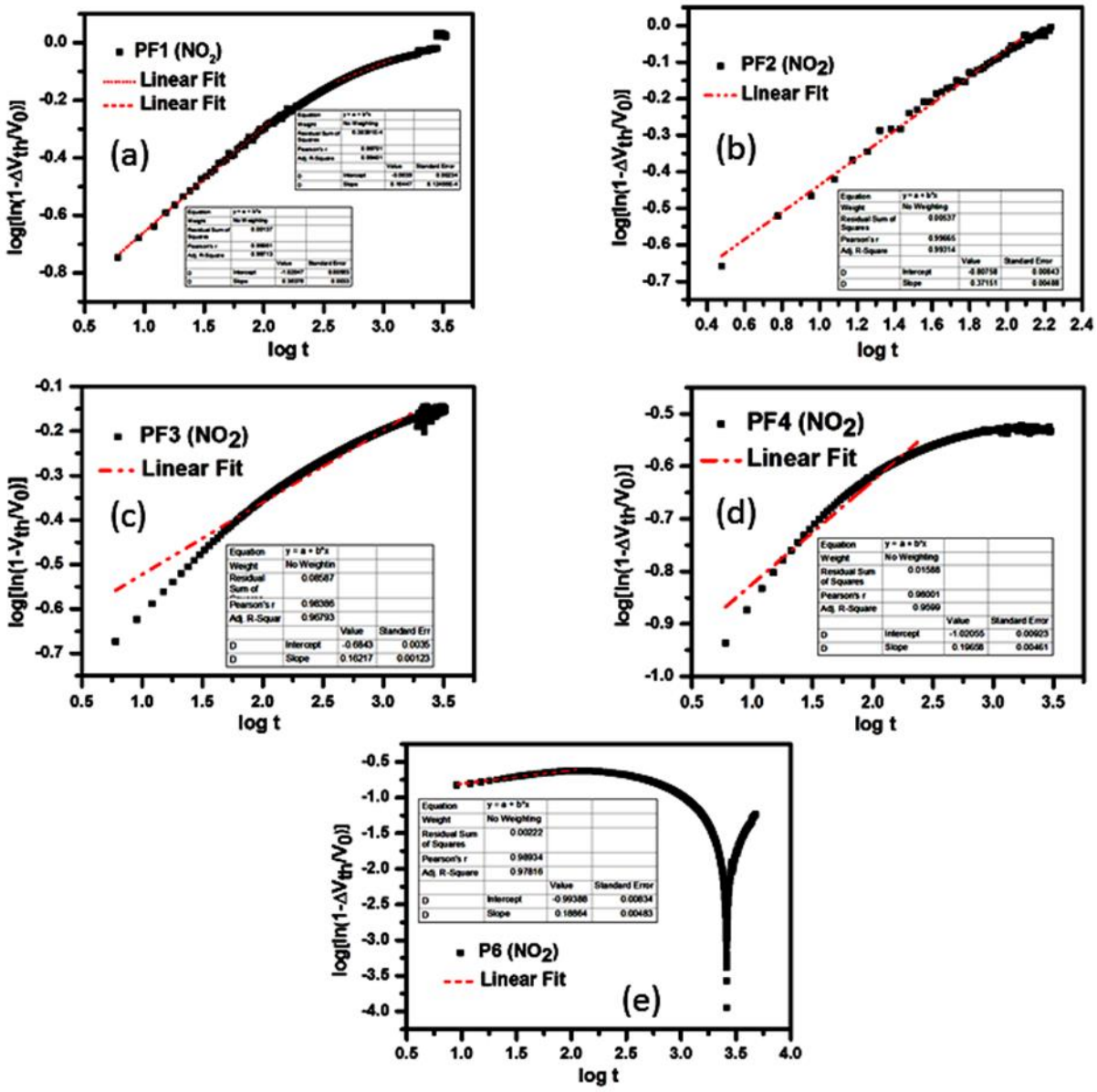

Figure S22. Elucidation of β and τ for V_G=V_D=-80 V under NH_3 atmosphere (10 ppm) (a) **PF1** (b) **PF2** (c) **PF3** (d) **PF4** (e) **P6**

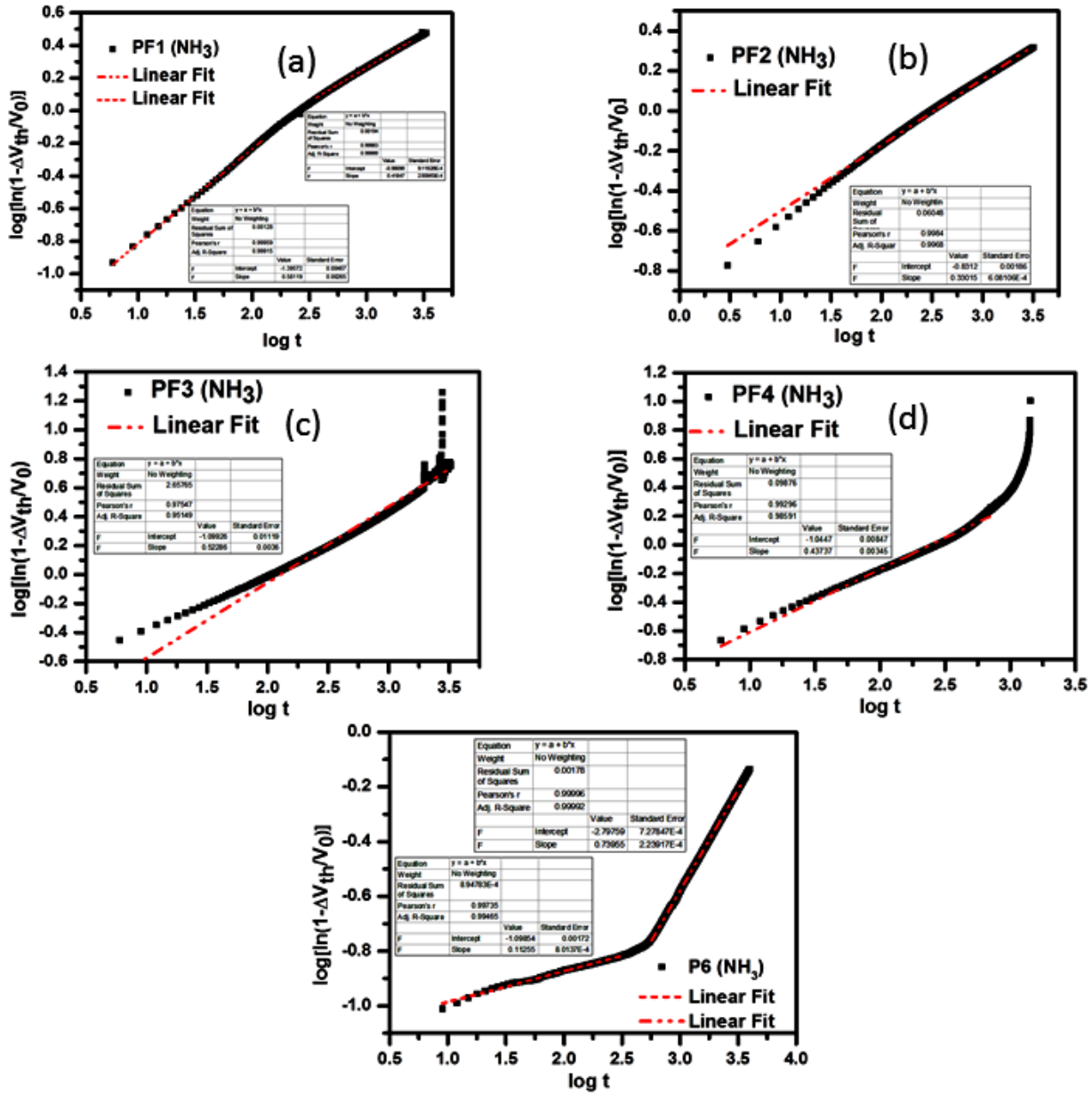

Figure S23. Elucidation of β and τ for V_G=V_D=-80 V under NH_3 atmosphere (10 ppm) (a) **PF1** (b) **PF2** (c) **PF3** (d) **PF4** (e) **P6**

Table S4. β values for gate bias under (i) NO_2 atmosphere (10 ppm) (ii) NH_3 atmosphere (10 ppm). (k_bT/β (eV) included in parenthesis)

Polymers	β(NO_2)	β(NH_3)
PF1	0.26 (0.11eV)	0.49 (0.06 eV)
PF2	0.37 (0.11 eV)	0.35 (0.08 eV)
PF3	0.19 (0.16 eV)	0.45 (0.07 eV)
PF4	0.20 (0.15 eV)	0.51 (0.06 eV)
P6	0.19 (0.15 eV)	0.42 (0.07 eV),0.73 (0.04 eV)

Table S5. V_{dipole} calculations for the bias stress phenomenon. Calculation of V_{dipole}:

We know that: $S = [kT \ln(10)/q] \times (1+C_D/C_{ox}) \rightarrow (1)$ On application of bias stress on the polymer sensor OFET; the subthreshold swing becomes: $S' = [kT \ln(10)/q] \times (1+ \{C_D+C_{it}\}/C_{ox}) \rightarrow (2)$ The difference between the subthreshold swings is given as S-S': $\Delta S (S-S') = (kT/q) \times \ln 10 \times C_{it}/C_{ox} \rightarrow (3)$ The interface state capacitance arises from the dipole created as a consequence of trapped charges, which causes the shifts in the threshold voltage, which is given as: $\Delta V_{th} = (C_{it}/C_{ox}) \times V_{dipole} \rightarrow (4)$ Combining equations (3) and (4) we get: $\Delta V_{th} = (qV_{dipole}/kT\ln 10) \times \Delta S \rightarrow (5)$. Equation (5) can be used for bias stress and reverse bias stress to evaluate the V_{dipole}. We consider the ΔV_{th} at t=0 minutes and at t=300 mins (post bias stress) and post reverse bias stress and the ΔS at t=0 minutes and at t=300 mins (post bias stress) and post reverse bias stress to evaluate the V_{dipole}.[3,4,5]

Polymer	ΔV_{th} (V)	ΔS (V/dec)	V_{dipole} (V)
PF1	69	10.25	0.404
PF2	65	28.67	0.134
PF3	53	11.3	0.280
PF4	47	2.7	0.117
P6	1.2	1.73	0.04

Table S6. V_{dipole} calculations for the reverse bias stress (trap erase) phenomenon

Polymer	ΔV_{th} (V)	ΔS (V/dec)	V_{dipole} (V)
PF1	26	20.83	0.050
PF2	21	17.6	0.071
PF3	33	18.47	0.106
PF4	23	32.7	0.042
P6	21	35.6	0.036

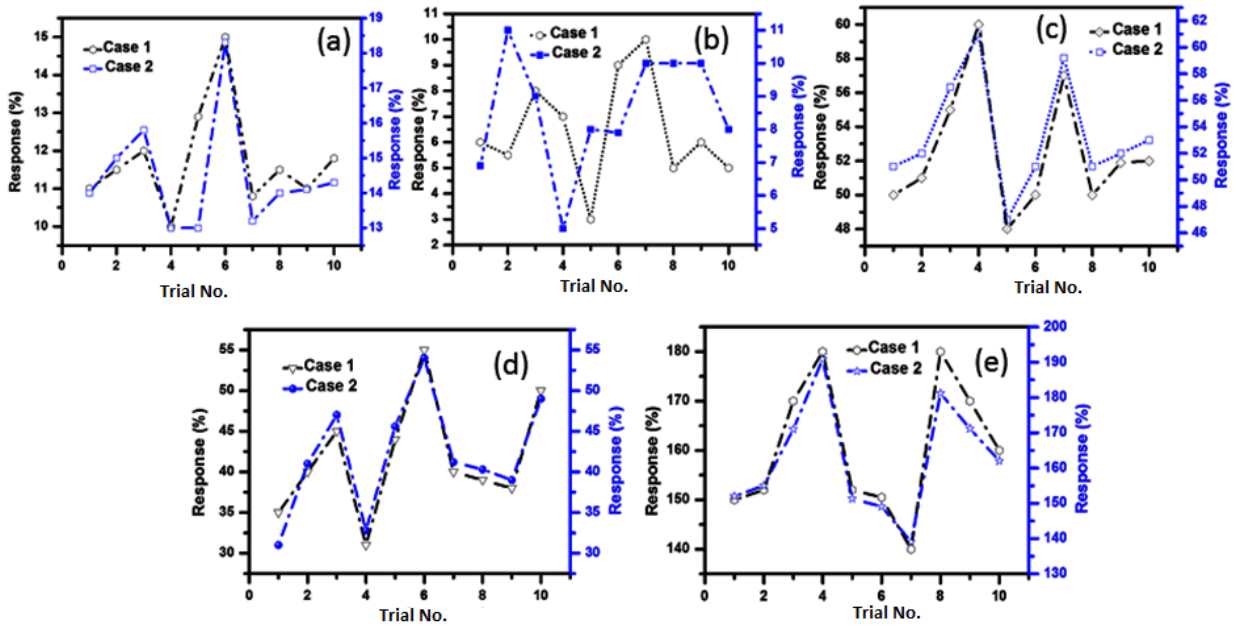

Figure S24. Responses to NO_2 (10 ppm) (monitored at V_G=-80 V for all polymers, collected from **Figure 10**). For every polymer, the first set represents responses after completion of the NO_2 aided recovery after gate bias application (V_G=V_D=-80 V, 5 hours) while the second set represents responses of independent devices (but of the same film for each trial) not subjected to gate bias and direct exposure to NO_2. (a)-(e): **PF1** to **P6**. For both the cases in case of each polymer, the exposure time was 5 minutes. For case 1 and case 2: the response corresponding to each trial number is an average from 10 separate devices each from a different film.

Table S7. Statistical calculation of t and p-values for the case in **Figure S24**.

Polymers	t-value	p-value (one-tailed)	Result
PF1	-4.06	0.000369	Significant
PF2	-2.449	0.012397	Significant
PF3	-0.51695	0.3058	Not significant
PF4	-0.12346	0.451557	Not significant
P6	-0.27316	0.393919	Not significant

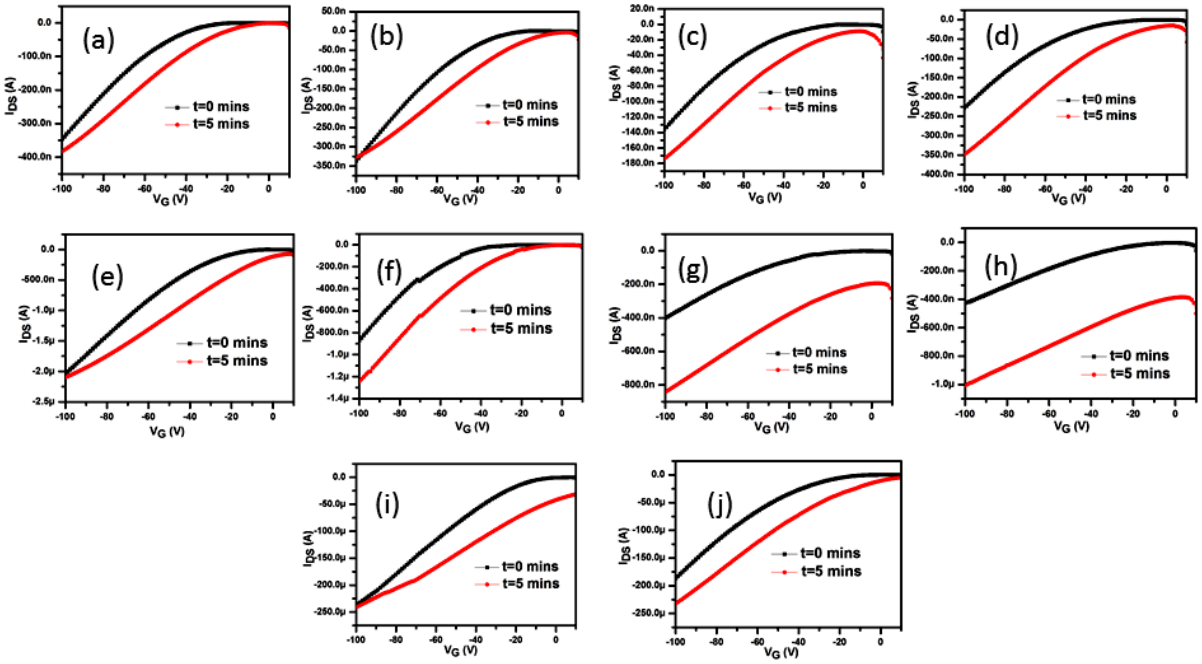

Figure S25. (a) **PF1** (t=0 mins represents the transfer curve after completion of recovery in air ~12 hours) and t=5 mins represents the transfer curve post exposure to 10 ppm of NO_2 for 5 minutes. (b) **PF1** (control, no bias stress, direct exposure, where t=0 mins represents transfer curve without the application of any gate bias, t=5 mins represents transfer curves after exposure to 10 ppm of NO_2 for 5 mins) (c) **PF2** (t=0 mins represents the transfer curve after completion of recover in air ~12 hours) and t=5 mins represents the transfer curve post exposure to 10 ppm of NO_2 for 5 minutes. (d) **PF2** (control, no bias stress, direct exposure, where t=0 mins represents transfer curve without the application of any gate bias, t=5 mins represents transfer curves after exposure to 10 ppm of NO_2 for 5 mins) (e) **PF3** (t=0 mins represents the transfer curve after completion of recover in air ~12 hours) and t=5 mins represents the transfer curve post exposure to 10 ppm of NO_2 for 5 minutes. (f) **PF3** (control, no bias stress, direct exposure, where t=0 mins represents transfer curve without the application of any gate bias, t=5 mins represents transfer curves after exposure to 10 ppm of NO_2 for 5 mins) (g) **PF4** (t=0 mins represents the transfer curve after completion of recovery in air ~12 hours) and t=5 mins represents the transfer curve post exposure to 10 ppm of NO_2 for 5 minutes. (h) **PF4** (control, no bias stress, direct exposure, where t=0 mins represents transfer curve without the application of any gate bias, t=5 mins represents transfer curves after exposure to 10 ppm of NO_2 for 5 mins) (i) **P6** (t=0 mins represents the transfer curve after completion of recover in air ~12 hours) and t=5 mins represents the transfer curve post exposure to 10 ppm of NO_2 for 5 minutes. (j) **P6** (control, no bias stress, direct exposure, where t=0 mins represents transfer curve without the application of any gate bias, t=5 mins represents transfer curves after exposure to 10 ppm of NO_2 for 5 mins. Condition: V_G=V_D=-80 V. *The responses have been monitored at V_G=-80 V (from transfer curves). Please note that we have provided the transfer curves for only the best device. The response data are an average from 10 devices, each from a different film.*

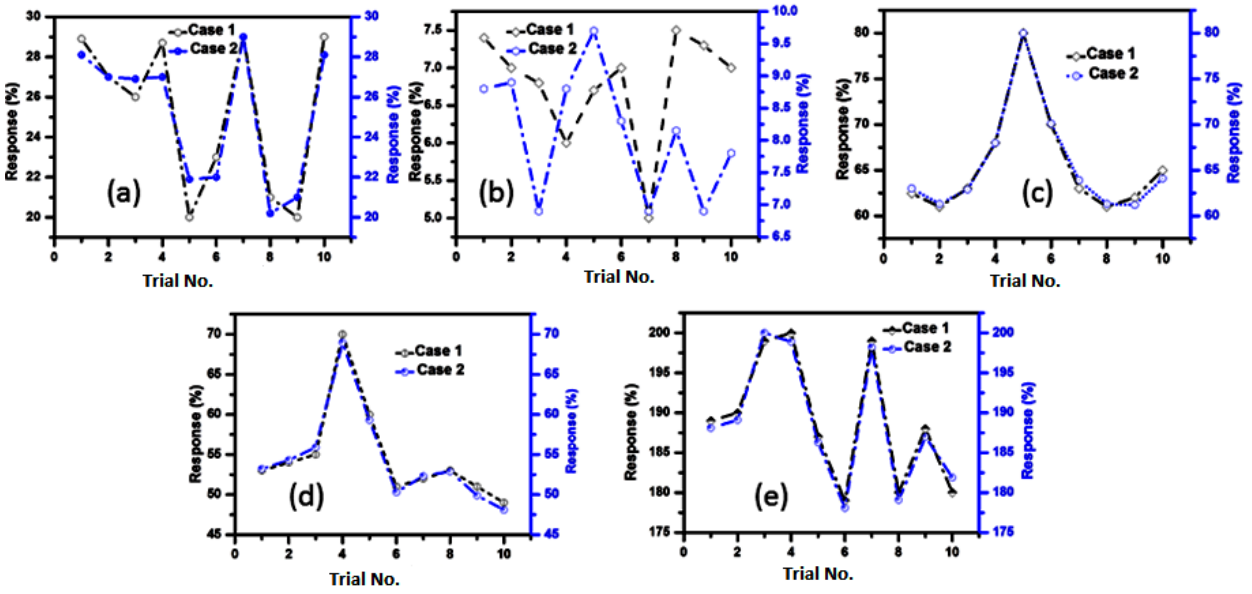

Figure S26. Responses to NO_2 (10 ppm). For every polymer, the first set represents responses after completion of the air aided recovery after gate bias application (V_G=V_D=-80 V) while the second set represents responses of independent devices not subjected to gate bias and direct exposure to NO_2. For both the cases in case of each polymer, the exposure time was 5 minutes. *Responses are monitored at V_G=-80 V.*

Table S8. Statistical calculation of t and p-values for the case in **Figure S26**.

Polymers	t-value	p-value (one tailed)	Result
PF1	0.08581	0.466282	Not significant
PF2	-3.44341	0.001449	Significant
PF3	-0.01333	0.494755	Not significant
PF4	0.010342	0.459388	Not significant
P6	0.11922	0.453211	Not significant

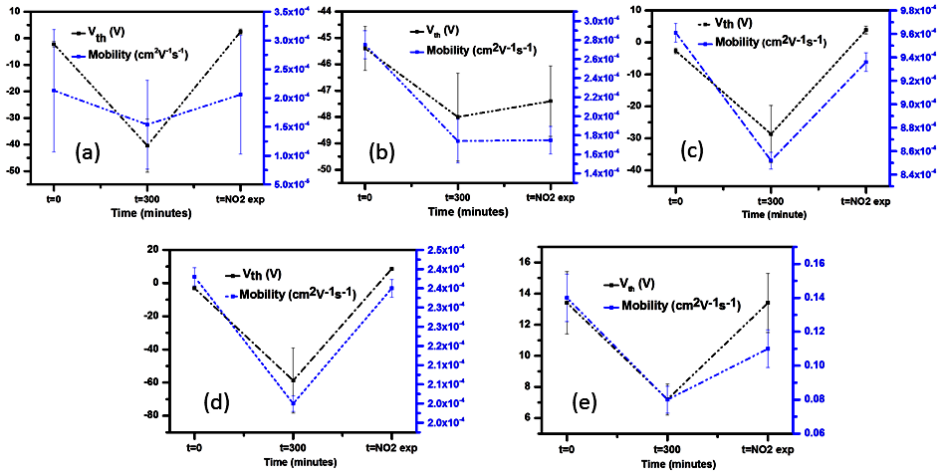

Figure S27. Changes in V_{th} and μ at t=0 mins (initial transfer characteristic), at t=300 mins (immediately after bias stress) and after continuous exposure to NO_2 to aid the recovery process. The recovery times are mentioned in the text.

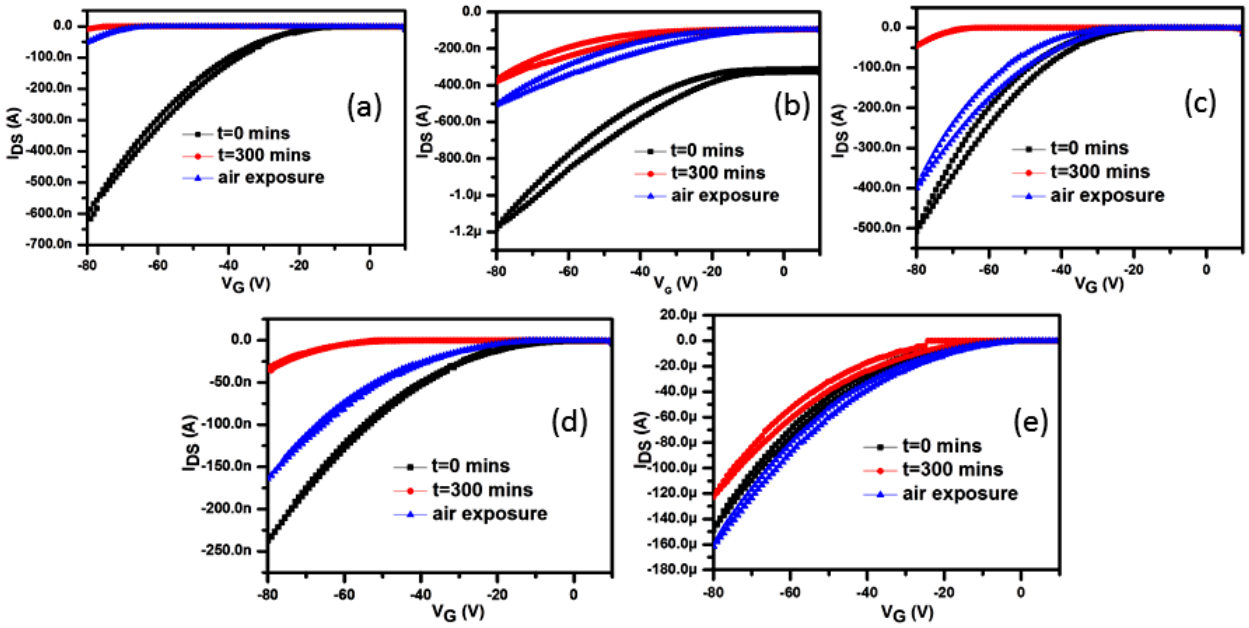

Figure S28. Transfer curves showing air aided recovery from gate bias (V_G=V_D=-80 V) for (a) **PF1** (b) **PF2** (c) **PF3** (d) **PF4** and (e) **P6** respectively. 16 mins, 25 mins, 18 mins, 15 mins, 10 mins for **PF1-P6** were the exposure times in air, respectively. The recovery can be explained as follows. Since organic semiconductors are permeable to water, water molecules can also reach the SiO_2 surface in the presence of an organic semiconductor. In this reaction, holes in the semiconductor are converted into proton which can be converted back into holes along with production of H_2. The reversible motion of protons in SiO_2 has been demonstrated by memory effects occurring in $Si/SiO_2/Si$ devices, where protons move through the SiO_2 from one Si layer to the other. In the presence of water, holes in the organic semiconductor, indicated below by OS+, can be converted into protons in the electrolytic reaction $2H_2O + 4OS^+ \rightarrow 4H^+ + O_2(g) + 4OS$, where OS refers to electrically neutral sites in the organic semiconductor. Next, protons can be converted back into holes in the reaction $2H^+ + 2OS \rightarrow 2OS^+ + H_2$ (g). There will be an equilibrium between the surface density $[OS^+]$ of holes in the semiconductor and the volume density $[H^+]$ of protons in the oxide at the interface with the semiconductor, leading to the linear relation $[H^+] = \alpha[OS^+]$, where the parameter α is a proportionality constant, which is determined by the reaction constants. Systematic tailoring of molecular and microstructural features determines the degree of shift in V_{th} as well as recovery. Further at such high voltages; less mobile states are accessible due to increase in microstructural disorder (created along with inherent traps) causing more shallow traps. During recovery, under application of a zero gate bias the transfer curve of a transistor that has suffered from bias stress shifts back to the transfer curve before the bias stress.

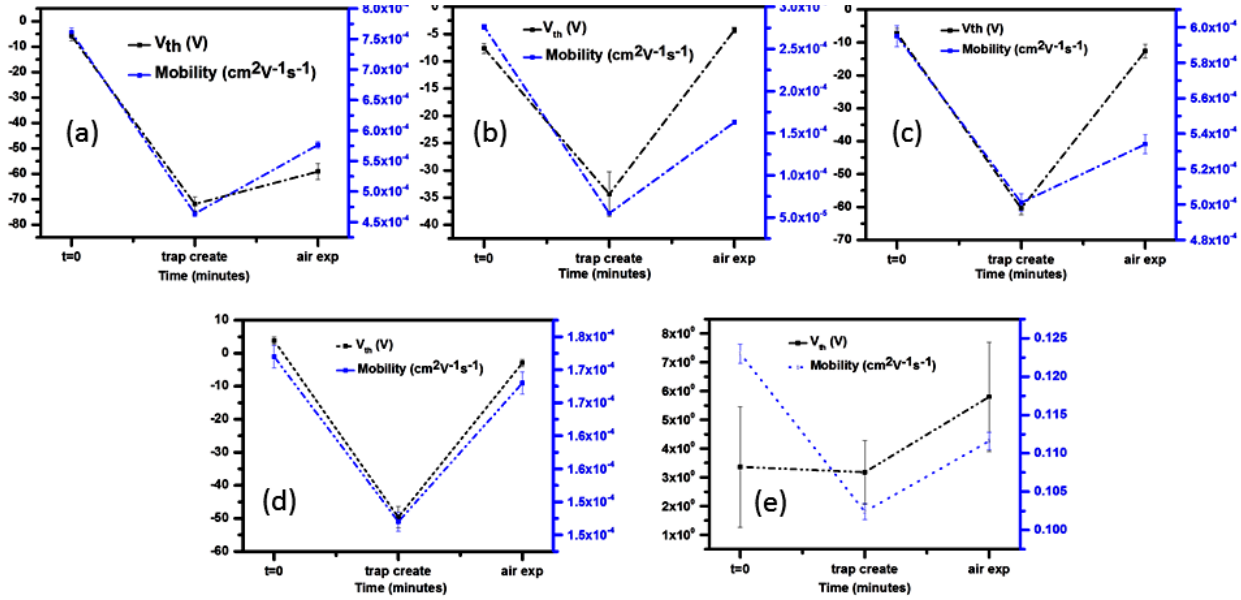

Figure S29. Changes in V_{th} and μ at t=0 mins (initial transfer characteristic), at the '**trap create**' time t=300 mins (immediately after bias stress) and after continuous **exposure to air** to aid the recovery process. The times for which the stressed devices were exposed to air (already mentioned in the main text) are 16, 25, 18, 15, 10 minutes.

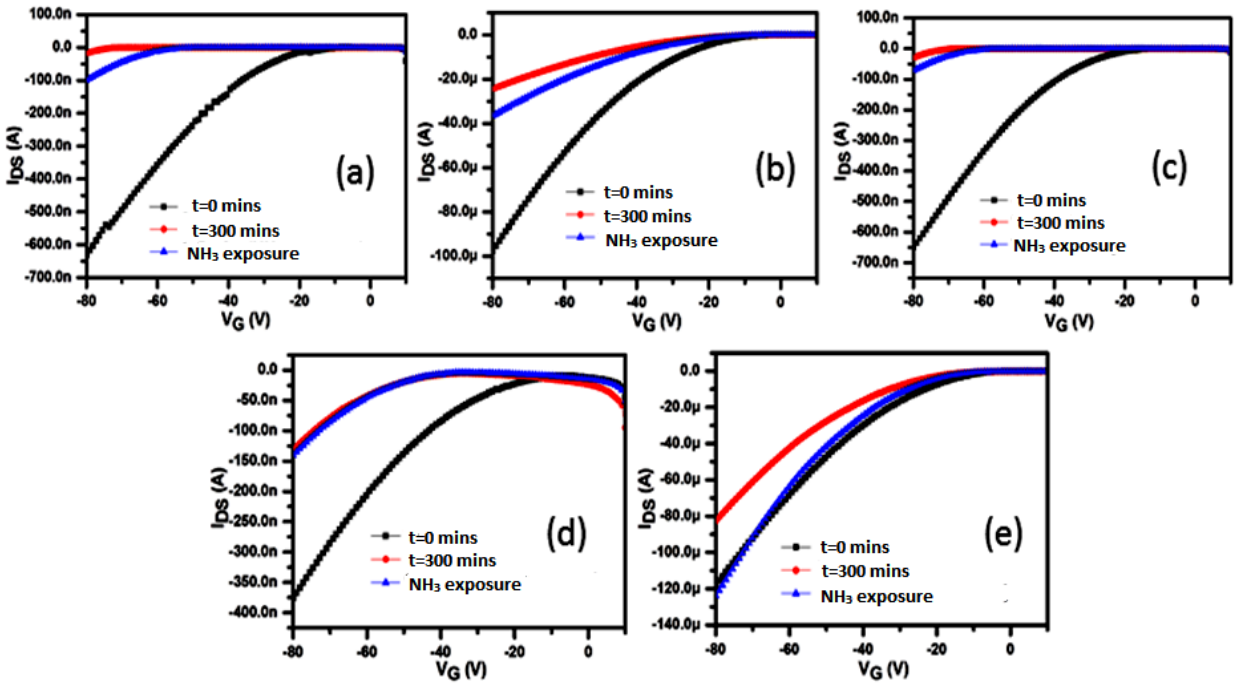

Figure S30. Transfer curves showing the effect of NH_3 gas (10 ppm) immediately after applying gate bias (V_G=V_D=-80 V, 300 mins) for (a) **PF1** (b) **PF2** (c) **PF3** (d) **PF4** and (e) **P6** respectively. The percentages are calculated at V_G=-80 V. The exposure times are:16 mins for **PF1**, 25 mins for **PF2**, 18 mins for **PF3**, 15 mins for **PF4** and 10 mins for **P6**.

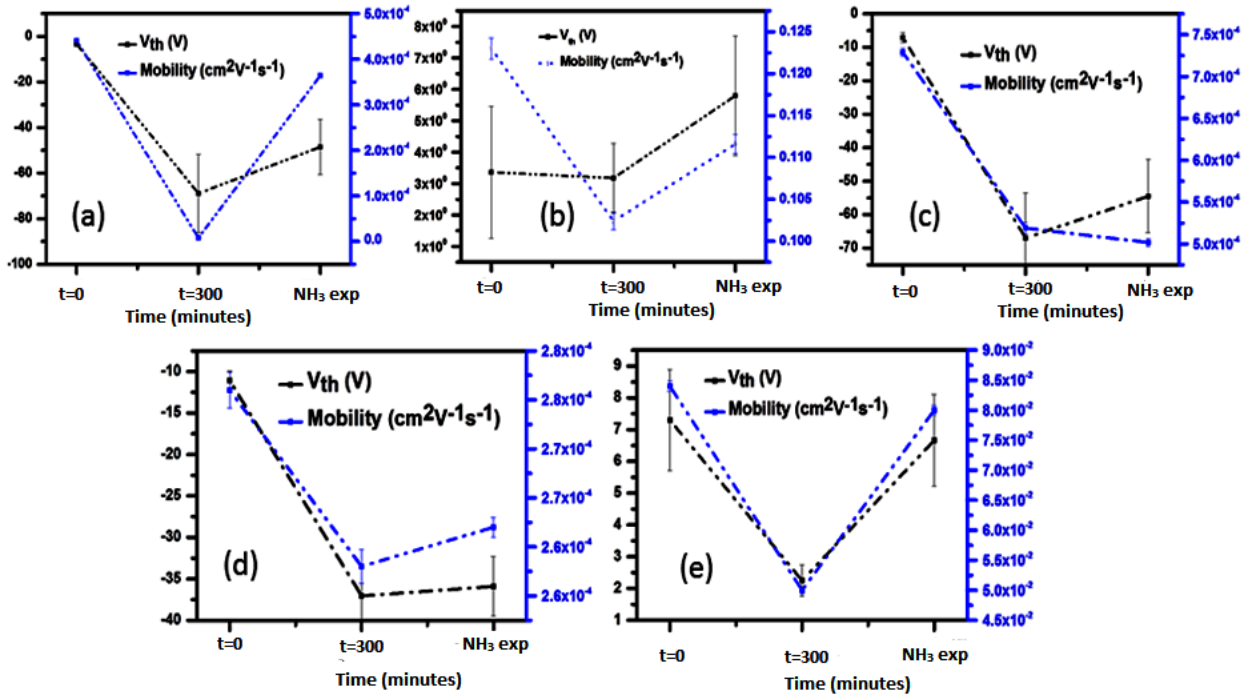

Figure S31. Changes in V_{th} and μ as an effect of NH_3 gas (10 ppm) immediately after applying gate bias (V_G=V_D=-80 V) for (a) **PF1** (b) **PF2** (c) **PF3** (d) **PF4** and (e) **P6** respectively. The percentages are calculated at V_G=-80 V. The exposure times are:16 mins for **PF1**, 25 mins for **PF2**, 18 mins for **PF3**, 15 mins for **PF4** and 10 mins for **P6**.

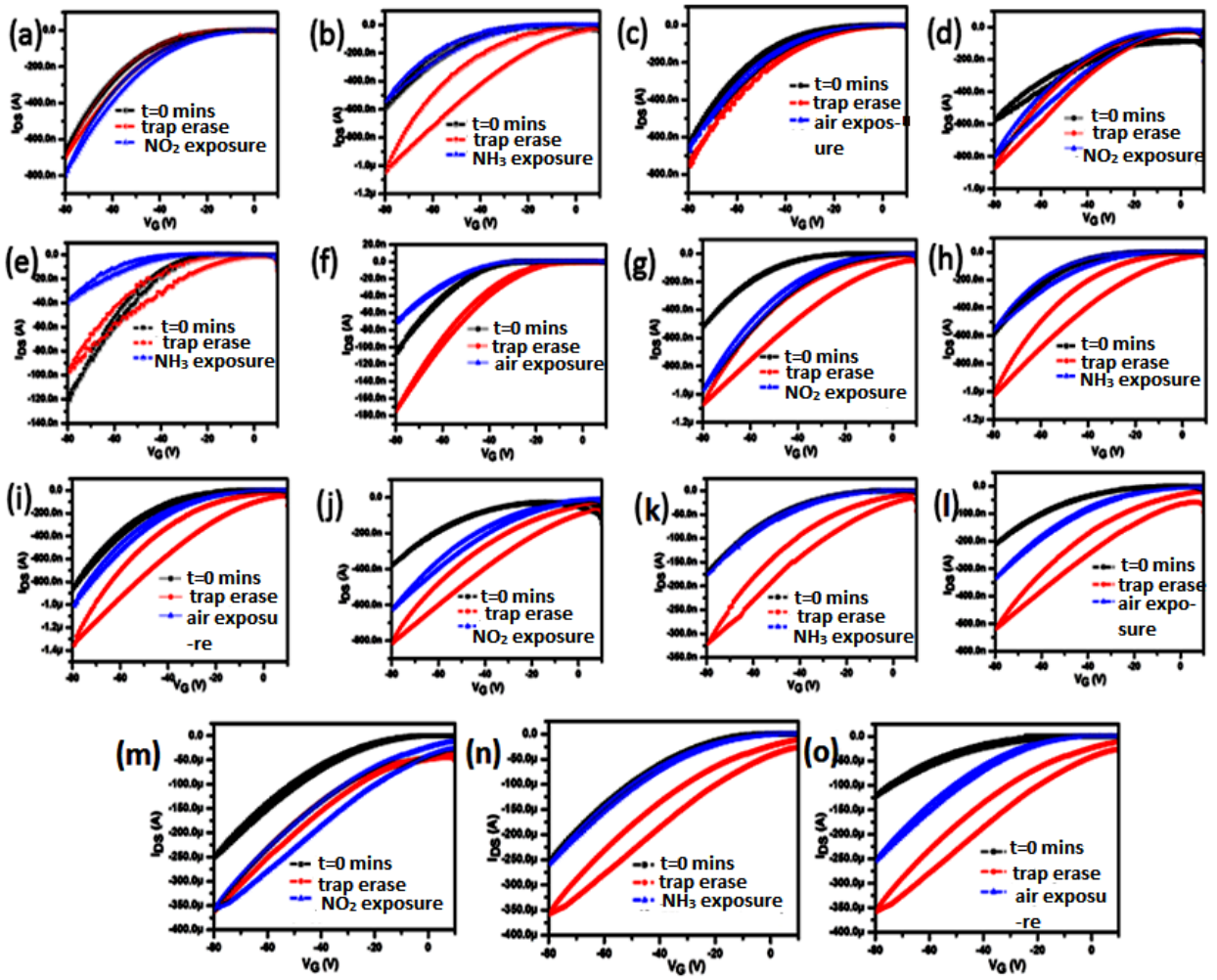

Figure S32. Transfer curves under ambient air (t=0 mins), post application of trap erase protocol [(i) (V_G=V_D=-80 V) and (ii) V_G = +80 V, V_D =0 V] followed by (a) 10 ppm NO_2 exposure for **PF1** (b) 10 ppm NH_3 exposure for **PF1** (c) ambient air exposure for **PF1** (d) 10 ppm NO_2 exposure for **PF2** (e) 10 ppm NH_3 exposure for **PF2** (f) ambient air exposure for **PF2** (g) 10 ppm NO_2 exposure for **PF3** (h) 10 ppm NH_3 exposure for **PF3** (i) ambient air exposure for **PF3** (j) 10 ppm NO_2 exposure for **PF4** (k) 10 ppm NH_3 exposure for **PF4** (l) ambient air exposure for **PF4** (m) 10 ppm NO_2 exposure for **P6** (n) 10 ppm NH_3 exposure for **P6** (o) ambient air exposure for **P6**. The exposure times are 16 mins for **PF1**, 25 mins for **PF2**, 18 mins for **PF3**, 15 mins for **PF4** and 10 mins for **P6**. Please note that only transfer curves for the best devices are shown; however, quantitative evaluation is done from 10 devices from independent, different films of every material.

Table S9. Trends in ΔV_{th} (V) and percent change of μ ($cm^2V^{-1}s^{-1}$) from reverse bias stress

Polymers	ΔV_{th} (V)	$\Delta\mu$ ($cm^2V^{-1}s^{-1}$)
PF1	26±5	123±1
PF2	21±3	100±2
PF3	33±5	147±54
PF4	23±2	97±2
P6	21±5	108±3

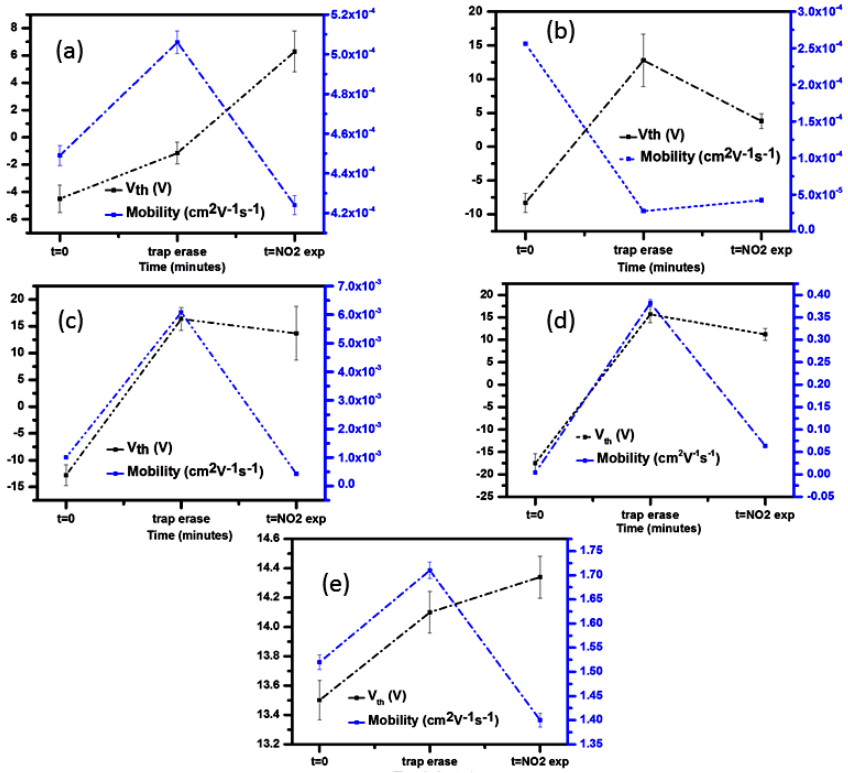

Figure S33. V_{th} and μ changes under ambient air (t=0 mins), post application of trap erase protocol [(i) (V_G=V_D=-80 V) and (ii) V_G = +80 V, V_D =0 V] followed by 10 ppm NO_2 exposure for (a) **PF1** (b) **PF2** (c) **PF3** (d) **PF4** (e) **P6.** The exposure times are 16 mins for **PF1**, 25 mins for **PF2**, 18 mins for **PF3**, 15 mins for **PF4** and 10 mins for **P6**

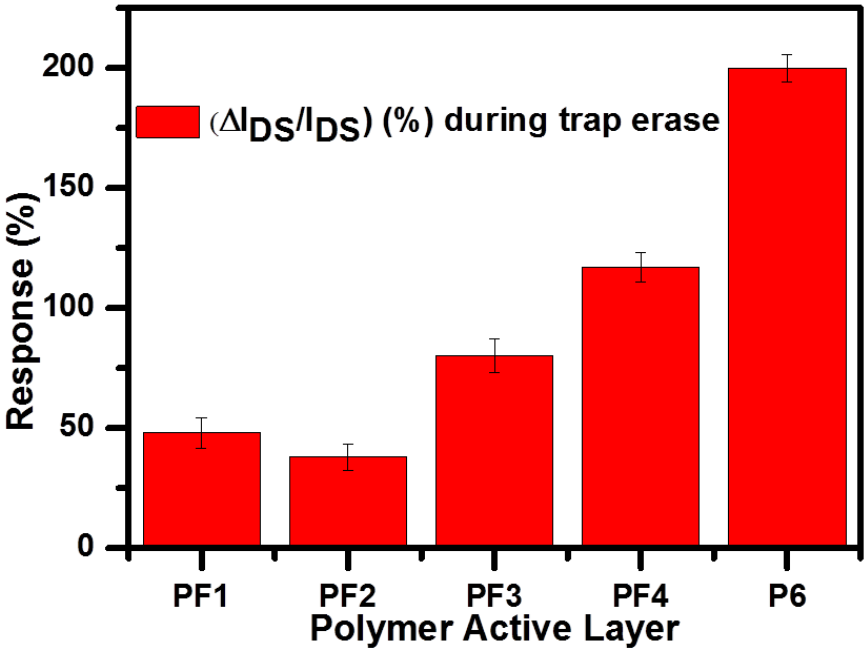

Figure S34. Change in I_{DS} (%) monitored at V_G=-80 V after trap erase. **P6** has highest mobility; so at V_G=-80 V, the current is the highest.

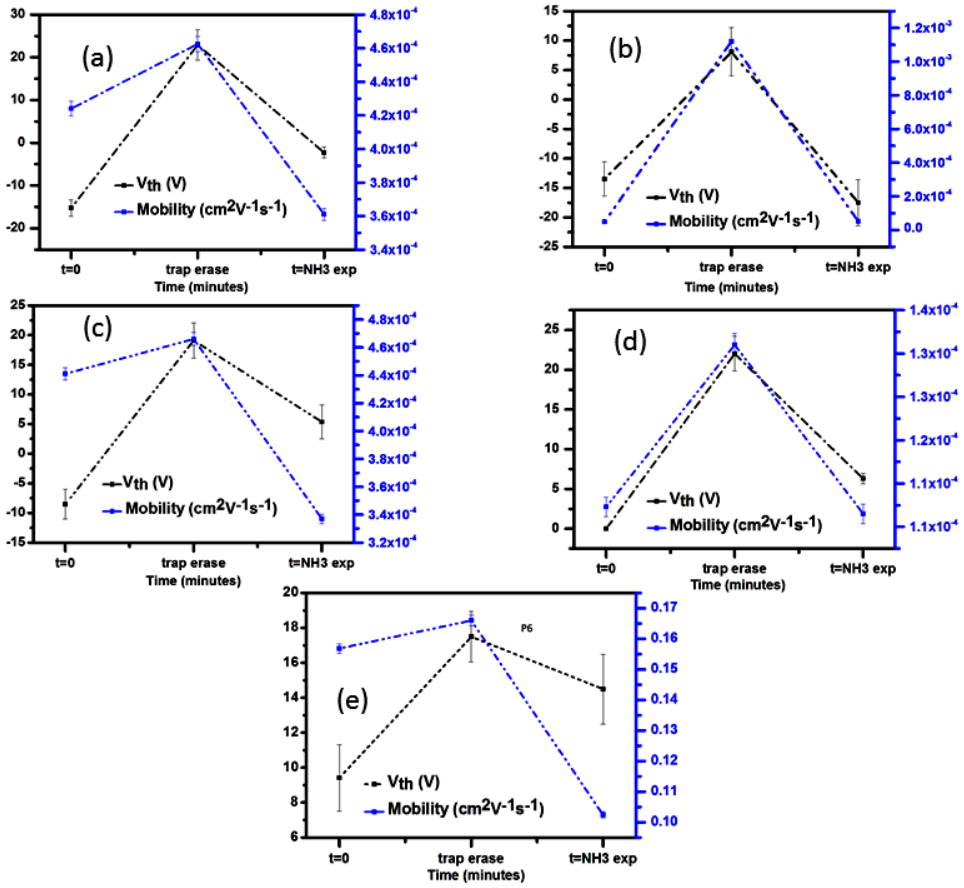

Figure S35. V_{th} and μ changes under ambient air (t=0 mins), post application of trap erase protocol [(i) (V_G=V_D=-80 V) and (ii) V_G = +80 V, V_D =0 V] followed by 10 ppm NH_3 exposure for (a) **PF1** (b) **PF2** (c) **PF3** (d) **PF4** (e) **P6.** The exposure times are 16 mins for **PF1**, 25 mins for **PF2**, 18 mins for **PF3**, 15 mins for **PF4** and 10 mins for **P6.**

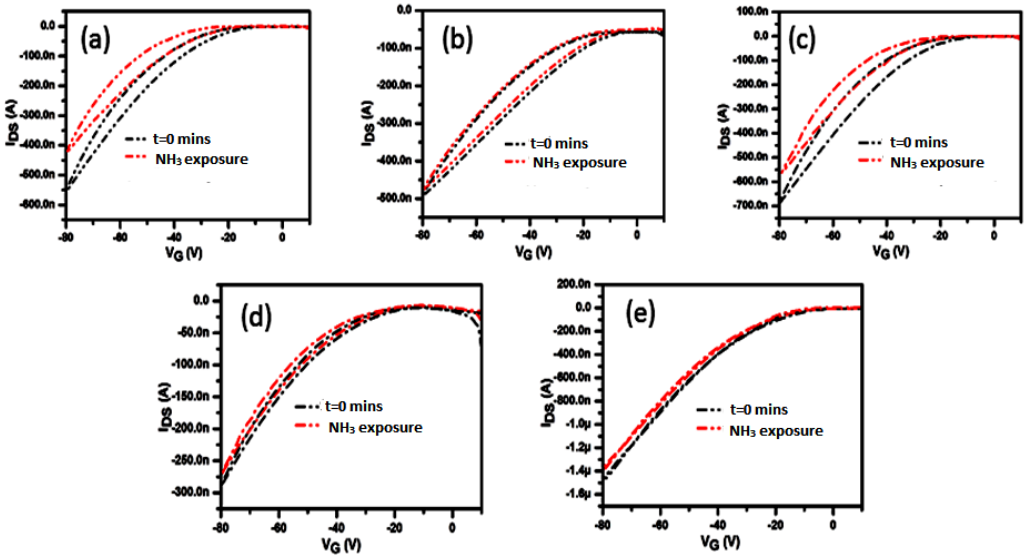

Figure S36. Transfer curves under ambient air (t=0 mins), and on exposure to 10 ppm of NH_3 (a) **PF1** (b) **PF2** (c) **PF3** (d) **PF4** (e) **P6.** This is a direct exposure of unstressed devices. These are the controls used for the trap erase experiments. The exposure times are 16 mins for **PF1**, 25 mins for **PF2**, 18 mins for **PF3**, 15 mins for **PF4** and 10 mins for **P6**

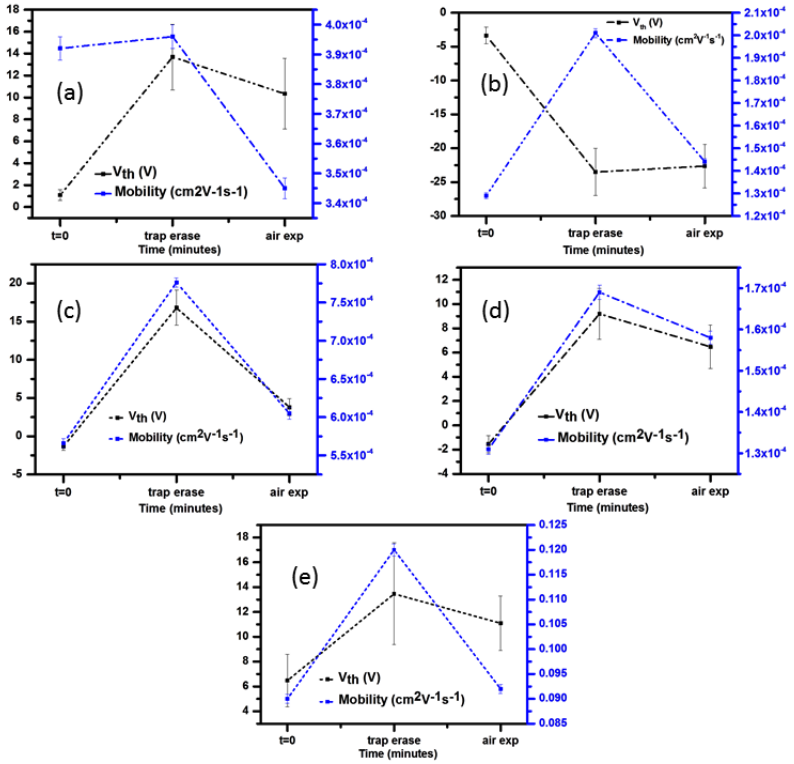

Figure S37. V_{th} and μ changes under ambient air (t=0 mins), post application of trap erase protocol [(i) (V_G=V_D=-80 V) and (ii) V_G = +80 V, V_D =0 V] followed by air exposure for (a) **PF1** (b) **PF2** (c) **PF3** (d) **PF4** (e) **P6.** The exposure times are 16 mins for **PF1**, 25 mins for **PF2**, 18 mins for **PF3**, 15 mins for **PF4** and 10 mins for **P6**

References:

(1) T. Mukhopadhyaya, J. S. Wagner, H. Fan, H. E. Katz, *ACS Appl. Mater. Interfaces,* 2020, **12**, 21974–21984.

(2) S. Y. Liu, M. M. Shi, J. C. Huang, Z. N. Jin, X. L. Hu, J. Y. Pan, H. Y. Li, A. K. Y. Jen, H. Z. Chen, *J. Mater. Chem. A*, 2013, **1**, 2795–2805.

(3) S. Vasudevan, N. Kapur, T. He, M. Neurock, J. M. Tour, A. W. Ghosh, *J. Appl. Phys.*, 2009, **105**, 093703. https://doi.org/10.1063/1.3091290.

(4) K. P. Pernstich, S. Haas, D. Oberhoff, C. Goldmann, D. J. Gundlach, B. Batlogg, A. N. Rashid, G. Schitter, *J. Appl. Phys.*, 2004, **96**, 6431. https://doi.org/10.1063/1.1810205.

(5) M. Salinas, C. M. Jäger, A. Y. Amin, P. O. Dral, T. Meyer-Friedrichsen, A. Hirsch, T. Clark, M. Halik, *J. Am. Chem. Soc*., 2012, **134,** 12648–12652.